Introduction to Computational Neuroscience

Biol 698
Math 635
Math 430

Bibliography:

"Mathematical Foundations of Neuroscience", by G. B. Ermentrout & D. H. Terman - Springer (2010), 1st edition. ISBN 978-0-387-87707-5

* "Dynamical Systems in Neuroscience: The Geometry of Excitability and Bursting", by Eugene M. Izhikevich. The MIT Press, 2007. ISBN 0-262-09043-8

Figures were taken from some of these books

Overview

Two-dimensional models

- Reduction of the Hodgkin-Huxley model to two-dimensional models (review)
- Two-dimensional neural models
- Two-dimensional dynamical systems
- Phase portraits and vector fields
- Equilibria and stability
- Bifurcations

Two-dimensional neural models

$$
\begin{aligned}
C\dot{V} &= I - \overbrace{\bar{g}_{\mathrm{K}} n^4 (V - E_{\mathrm{K}})}^{I_{\mathrm{K}}} - \overbrace{\bar{g}_{\mathrm{Na}} m^3 h (V - E_{\mathrm{Na}})}^{I_{\mathrm{Na}}} - \overbrace{g_{\mathrm{L}} (V - E_{\mathrm{L}})}^{I_{\mathrm{L}}} \\
\dot{n} &= (n_\infty(V) - n)/\tau_n(V) \, , \\
\dot{m} &= (m_\infty(V) - m)/\tau_m(V) \, , \\
\dot{h} &= (h_\infty(V) - h)/\tau_h(V) \, ,
\end{aligned}
$$

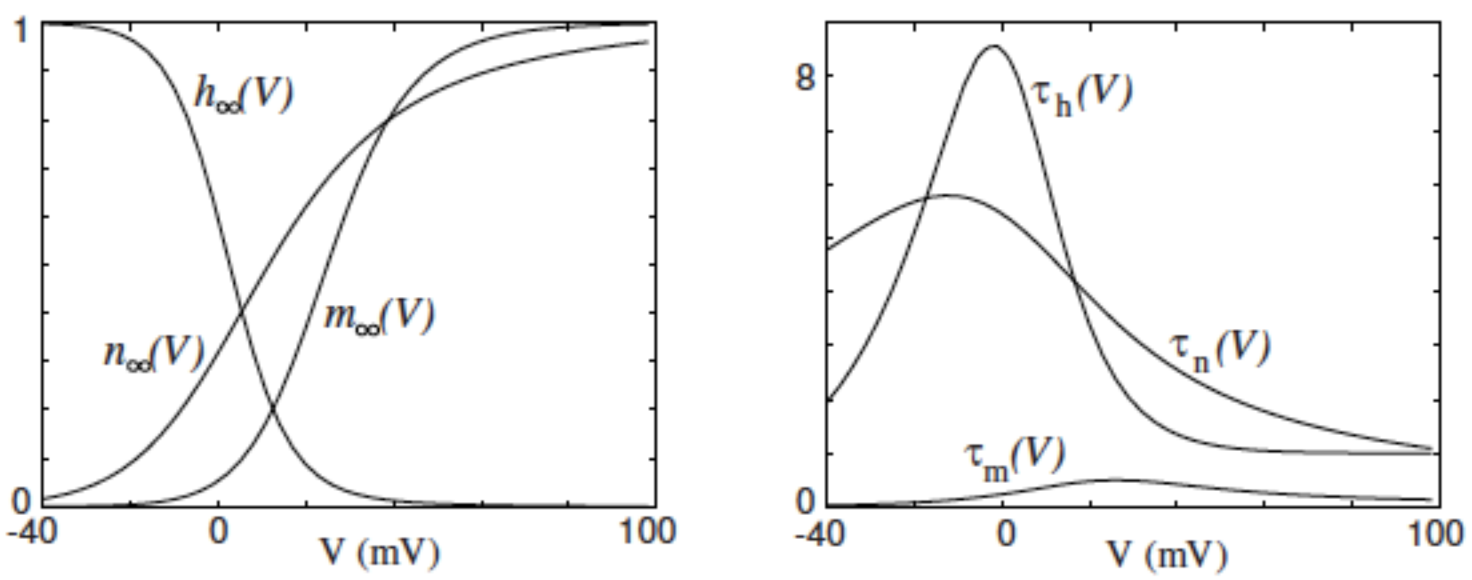

Figure 2.13: Steady-state (in)activation functions (left) and voltage-dependent time constants (right) in the Hodgkin-Huxley model.

Two-dimensional neural models

$$C\dot{V} = I - \overbrace{\bar{g}_K n^4 (V - E_K)}^{I_K} \overbrace{- \bar{g}_{Na} m^3 h (V - E_{Na})}^{I_{Na}} \overbrace{- g_L (V - E_L)}^{I_L}$$

$$\dot{n} = (n_\infty(V) - n)/\tau_n(V) \,,$$

$$\dot{m} = (m_\infty(V) - m)/\tau_m(V) \,,$$

$$\dot{h} = (h_\infty(V) - h)/\tau_h(V) \,,$$

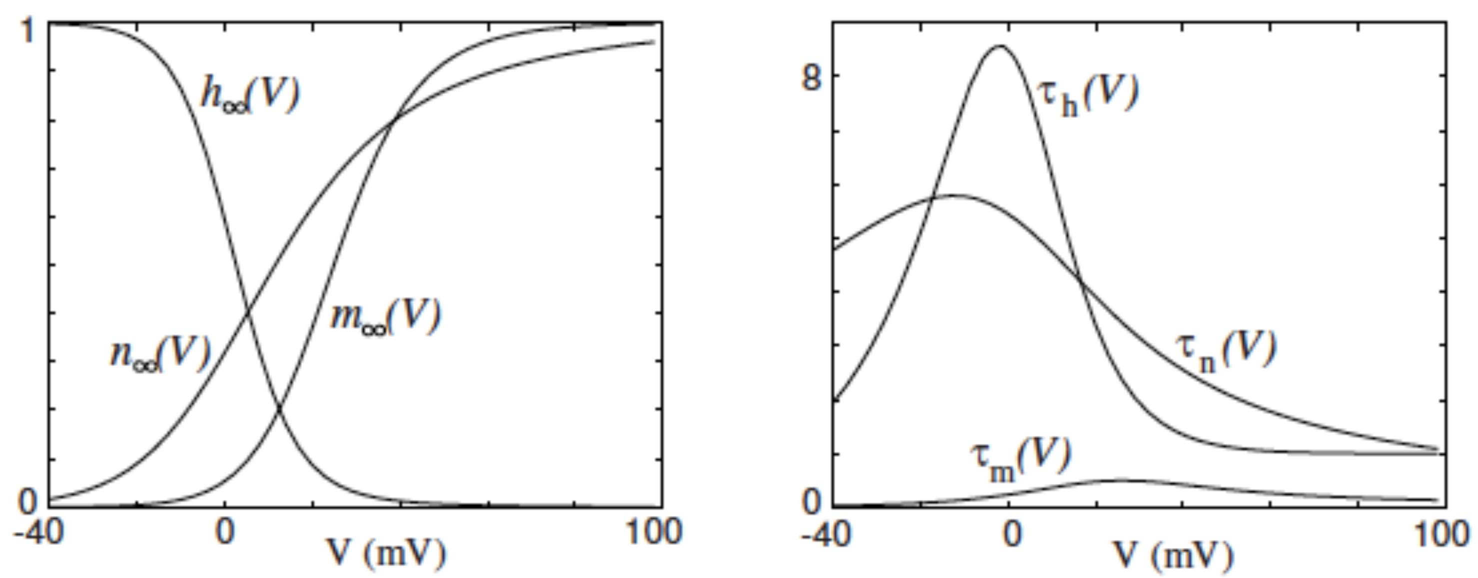

Figure 2.13: Steady-state (in)activation functions (left) and voltage-dependent time constants (right) in the Hodgkin-Huxley model.

Two-dimensional neural models

$$C\dot{V} = I - \overbrace{\bar{g}_{\mathrm{K}} n^4 (V - E_{\mathrm{K}})}^{I_{\mathrm{K}}} - \overbrace{\bar{g}_{\mathrm{Na}} m^3 h (V - E_{\mathrm{Na}})}^{I_{\mathrm{Na}}} - \overbrace{g_{\mathrm{L}} (V - E_{\mathrm{L}})}^{I_{\mathrm{L}}}$$

$$\dot{n} = (n_\infty(V) - n)/\tau_n(V)\,,$$

$$\dot{m} = (m_\infty(V) - m)/\tau_m(V)\,,$$

$$\dot{h} = (h_\infty(V) - h)/\tau_h(V)\,,$$

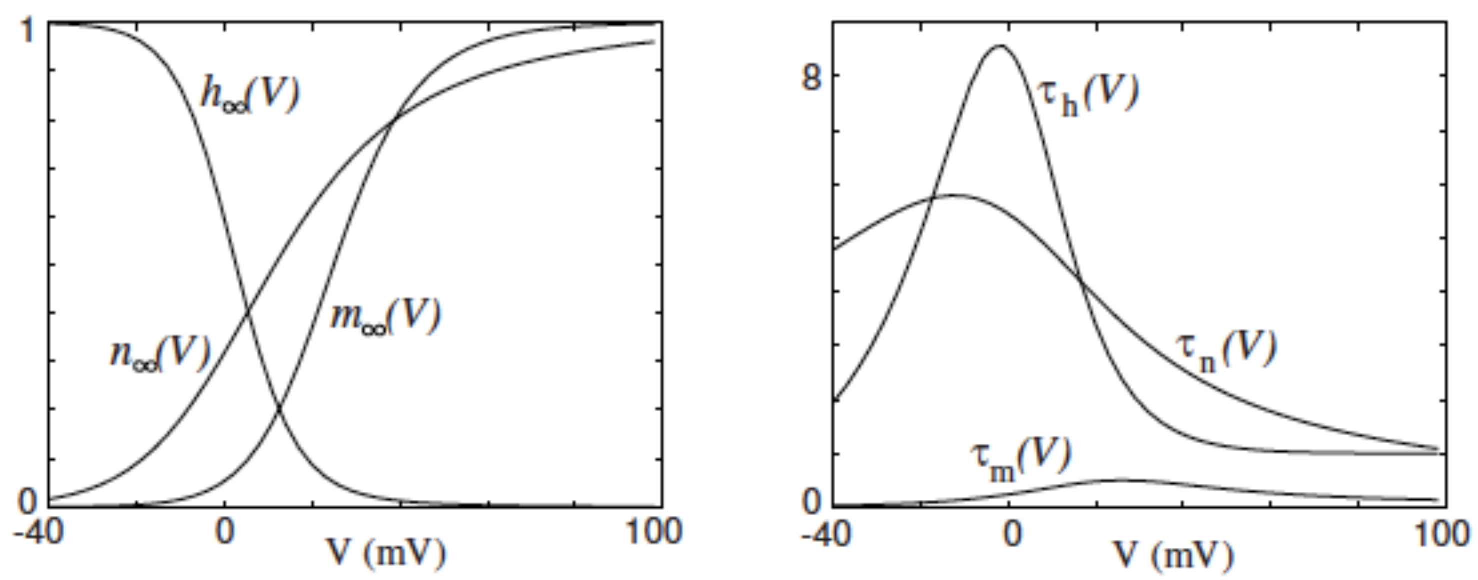

Figure 2.13: Steady-state (in)activation functions (left) and voltage-dependent time constants (right) in the Hodgkin-Huxley model.

Two-dimensional neural models

- Persistent sodium & potassium model

$$C\frac{dV}{dt} = - G_{Na} m_{\infty}{}^{3}(V)\,(V - E_{Na}) - G_K n^4\,(V - E_K) -$$
$$- G_L\,(V - E_L) + I_{app}$$

$$\frac{dn}{dt} = \frac{n_{\infty}(V) - n}{\tau_n(V)}$$

Two-dimensional neural models

- Persistent sodium & potassium model

$$C\frac{dV}{dt} = - G_{Na} p_{\infty}^{3}(V)\,(V - E_{Na}) - G_K n^4\,(V - E_K) -$$

$$- G_L\,(V - E_L) + I_{app}$$

$$\frac{dn}{dt} = \frac{n_{\infty}(V) - n}{\tau_n(V)}$$

Two-dimensional neural models

- Morris-Lecar model

$$C\frac{dV}{dt} = - G_{Ca} m_{\infty}(V)\,(V - E_{Ca}) - G_K w\,(V - E_K) -$$

$$- G_L\,(V - E_L) + I_{app}$$

$$\frac{dw}{dt} = \frac{w_{\infty}(V) - w}{\tau_w(V)}$$

Two-dimensional neural models

- Morris-Lecar model

$$m_\infty(V) = 0.5\left(1 + \tanh\frac{V + 1}{15}\right)$$

$$w_\infty(V) = 0.5\left(1 + \tanh\frac{V}{30}\right)$$

$$\tau_w(V) = \frac{5}{\cosh(V/60)}$$

Two-dimensional neural model

- FitzHugh-Nagumo (FHN) model

$$\frac{dV}{dt} = V - \frac{V^3}{3} - W + I$$

$$\frac{dW}{dt} = \phi (V + a - bW)$$

$a,\ b,\ \phi$: dimensionless & positive

ϕ ($\ll$ 1): inverse of a time constant

Two-dimensional neural models

- Quadratic integrate-and-fire model

$$\frac{dV}{dt} = I + V^2 \qquad \text{if } V \geq V_{peak}\text{, then } V \leftarrow V_{reset}$$

$$\text{Equilibria:} \quad V_{rest} = -\sqrt{I} \quad \text{and} \quad V_{thresh} = +\sqrt{I}$$

Bifurcations

- Saddle-node

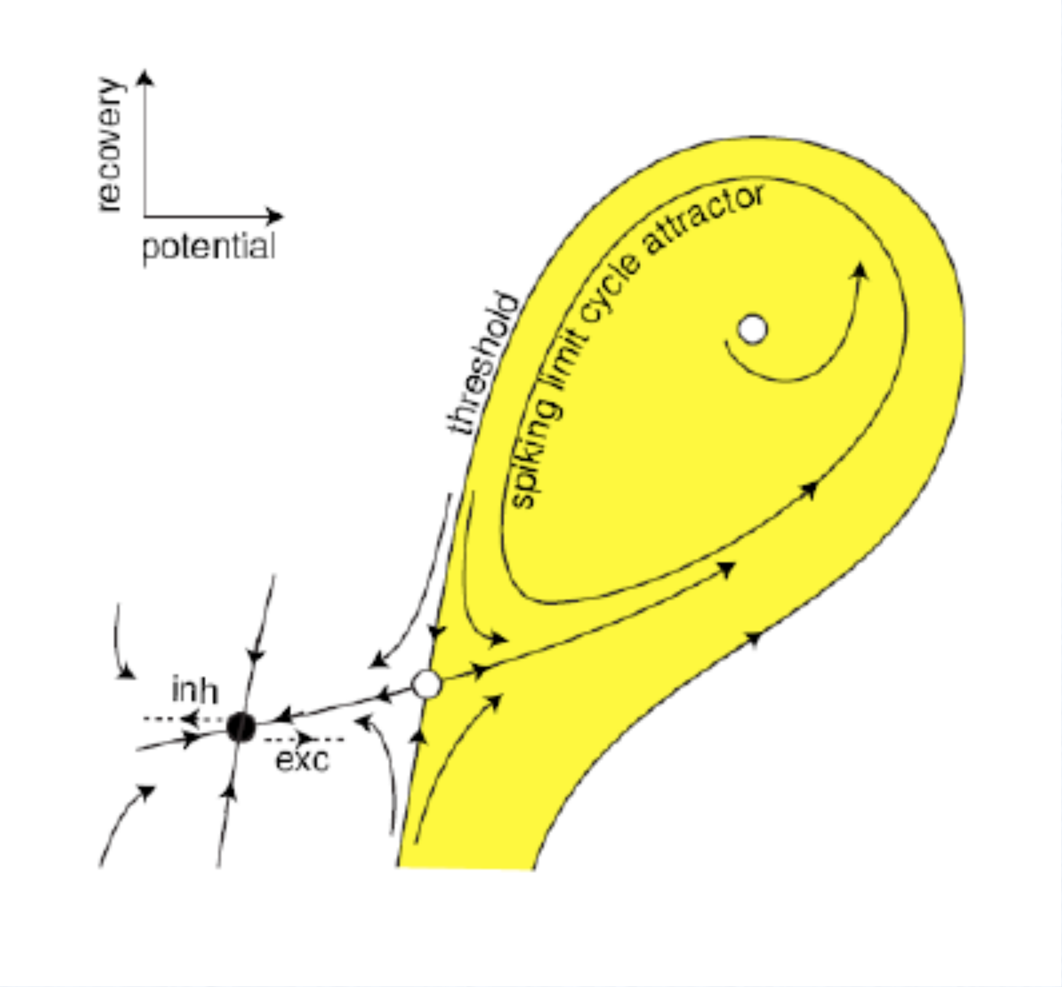

Bifurcations

- Saddle-node on an invariant circle (SNIC)

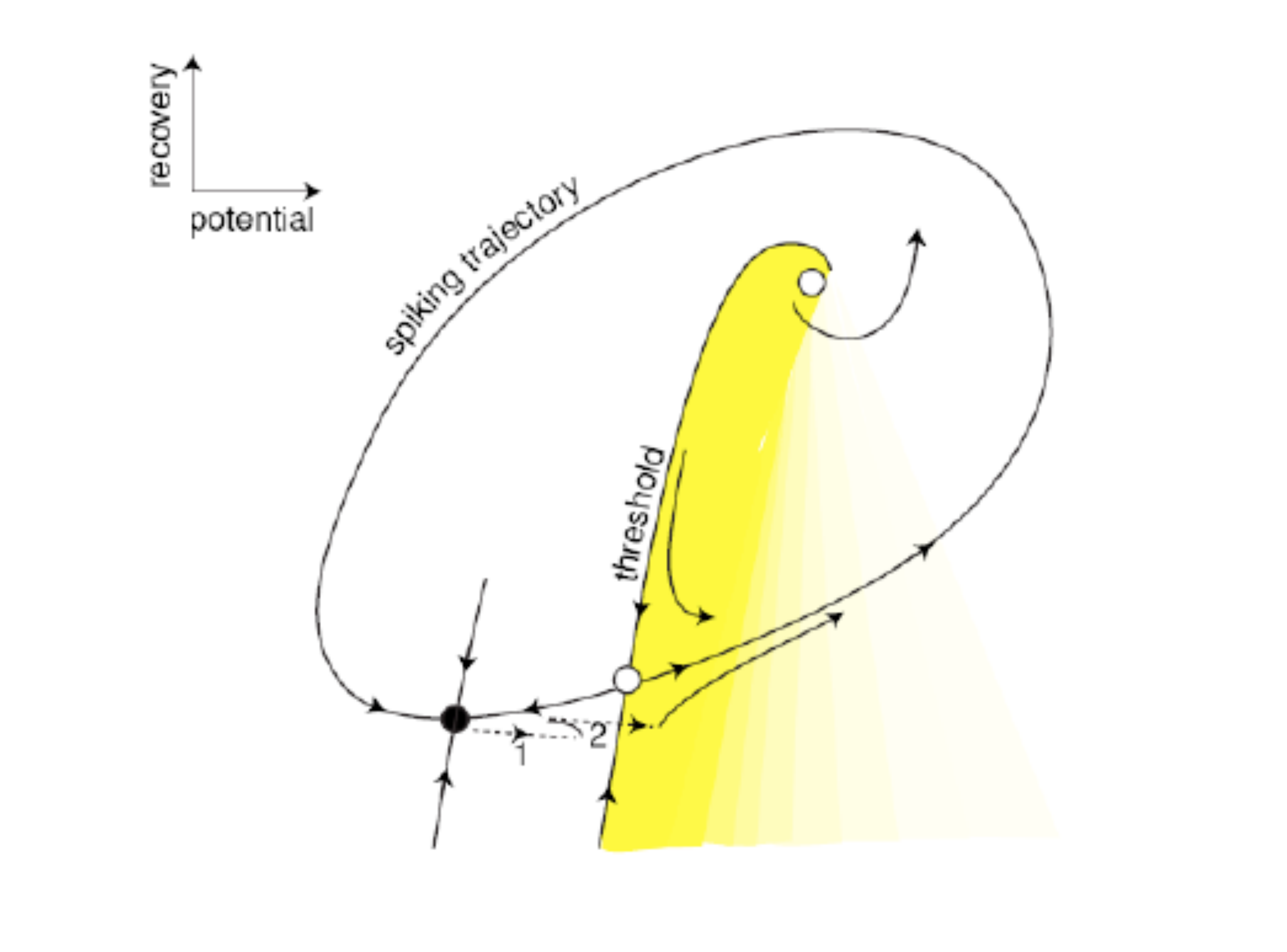

Bifurcations

- Subcritical Hopf (Andronov-Hopf)

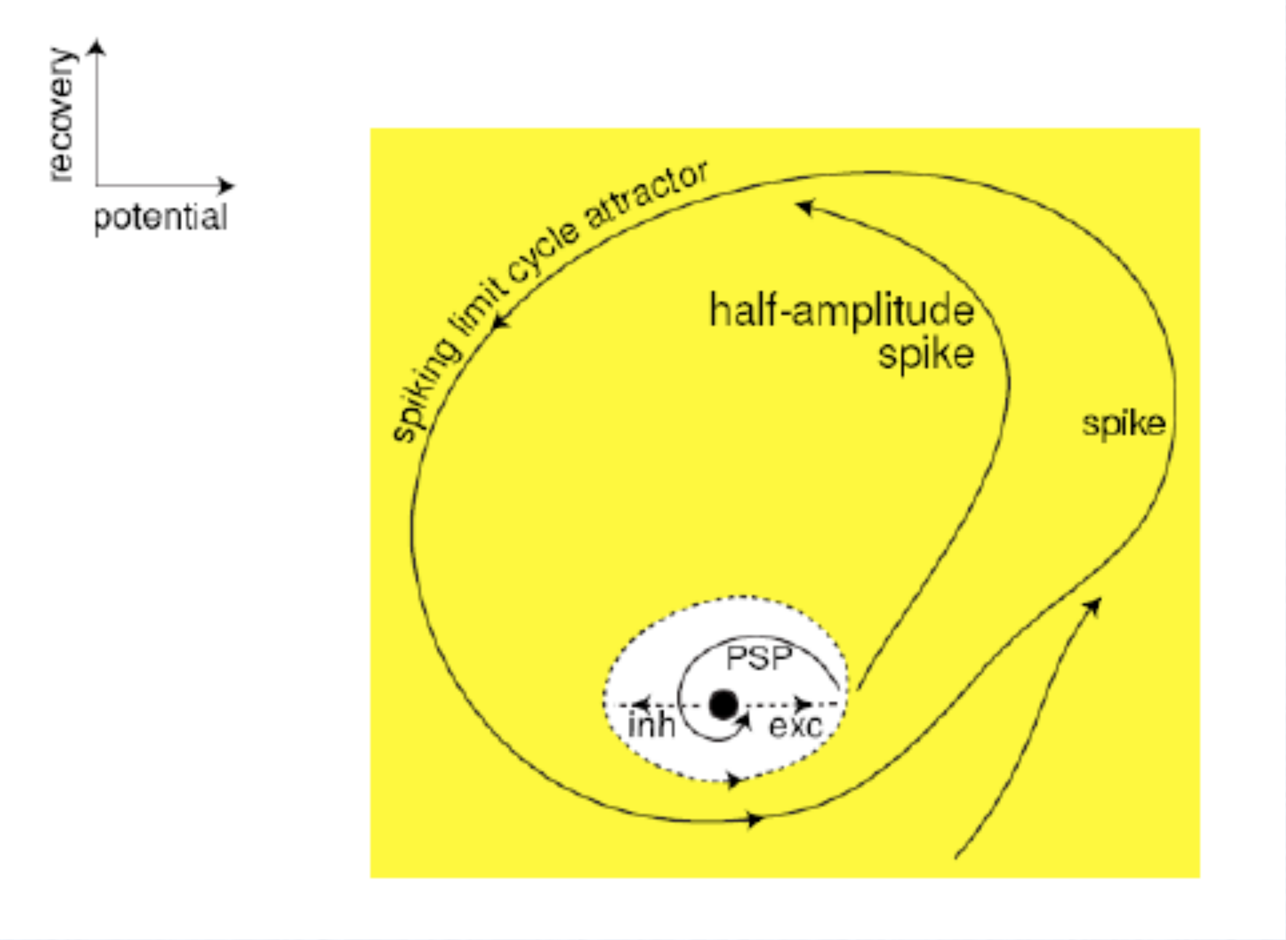

Bifurcations

- Supercritical Hopf (Andronov-Hopf)

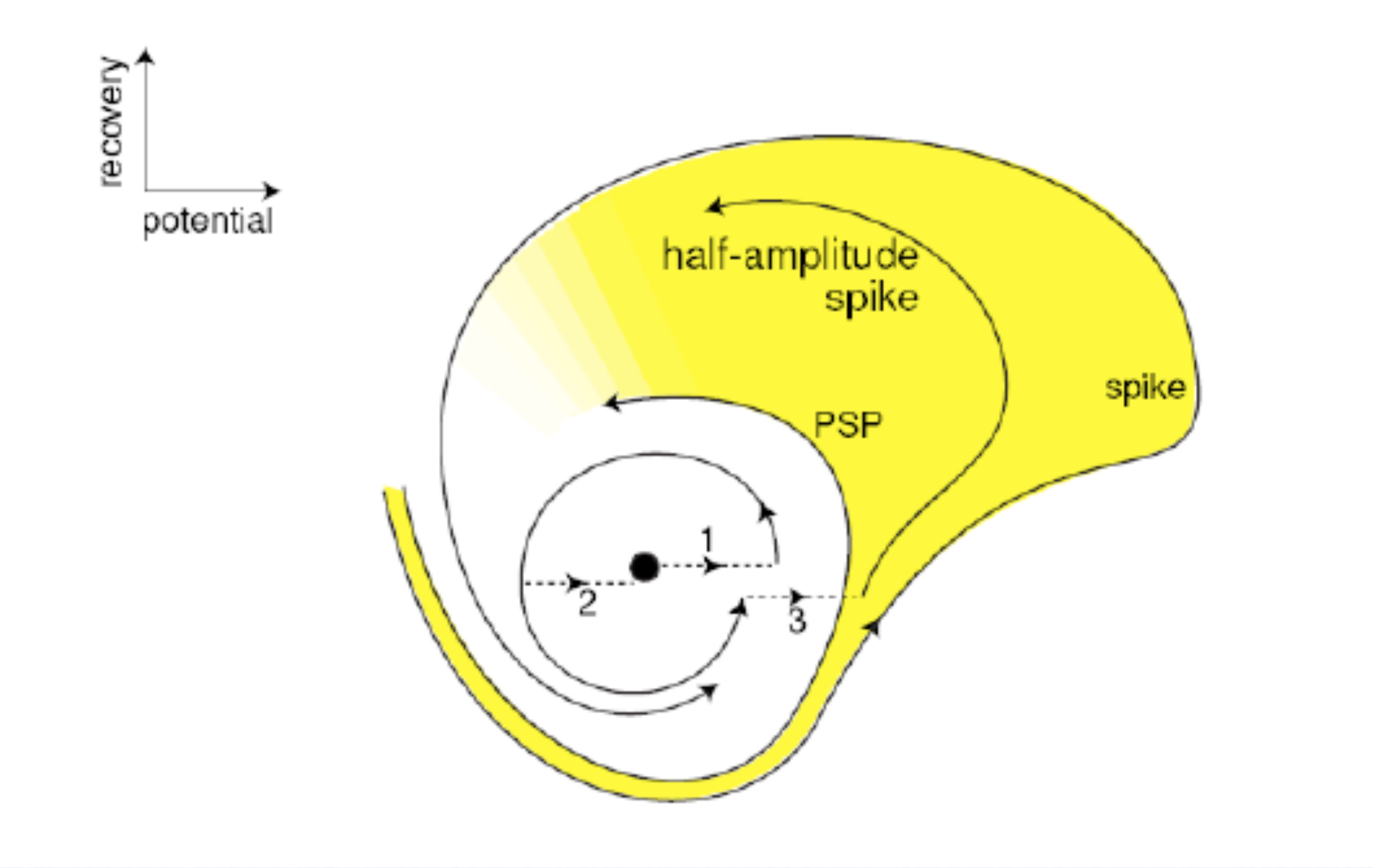

Two-dimensional dynamical systems

$$\frac{dx}{dt} = f(x, y) \qquad x(0) = x_0$$

$$\frac{dy}{dt} = g(x, y) \qquad y(0) = y_0$$

Two-dimensional dynamical systems

$$\frac{dx}{dt} = 1, \qquad \frac{dy}{dt} = 0$$

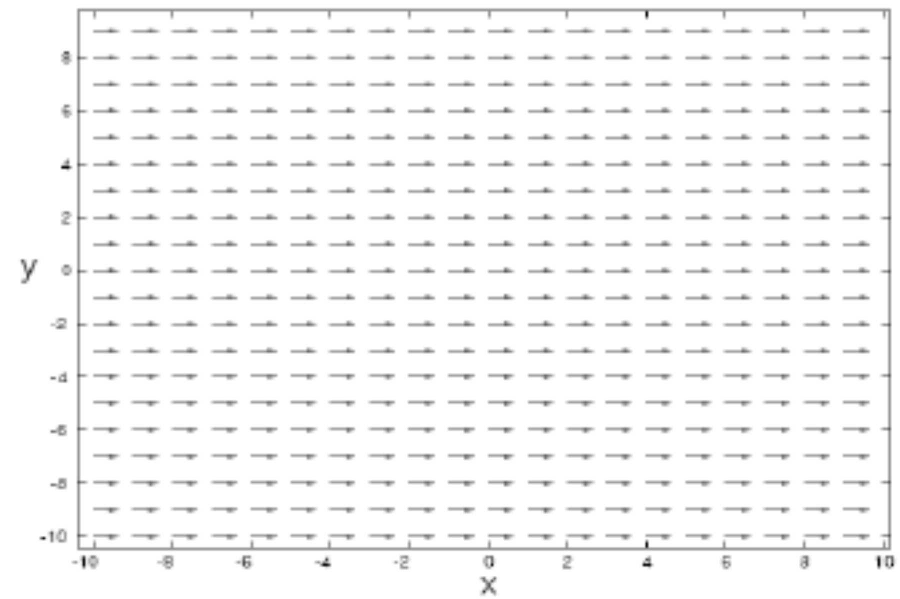

Two-dimensional dynamical systems

$$\frac{dx}{dt} = 0, \qquad \frac{dy}{dt} = 1$$

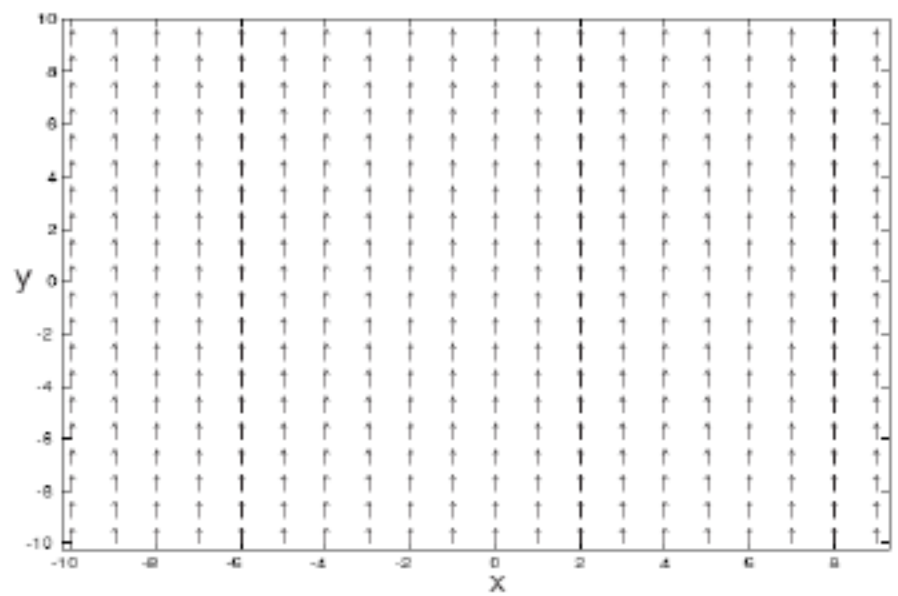

Two-dimensional dynamical systems

$$\frac{dx}{dt} = -x, \qquad \frac{dy}{dt} = -y$$

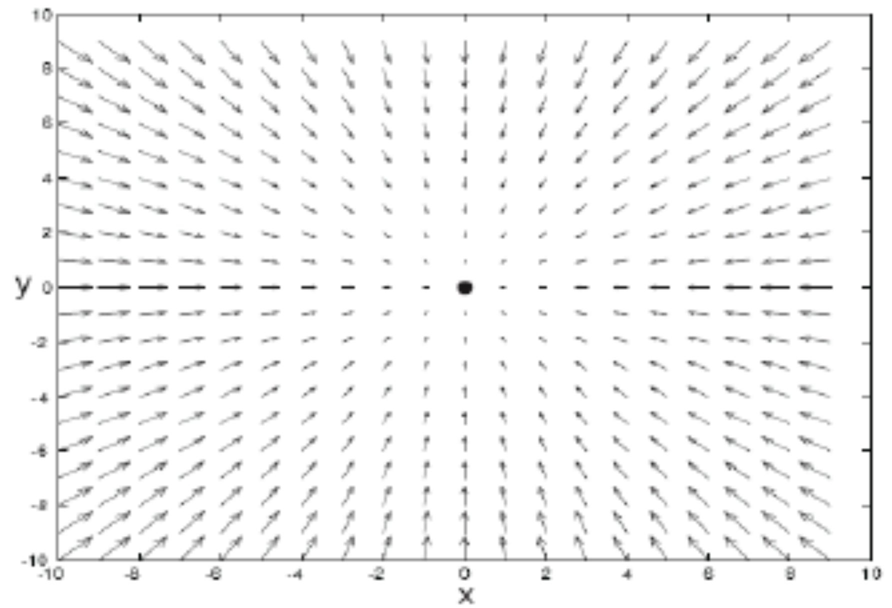

Two-dimensional dynamical systems

$$\frac{dx}{dt} = -y, \qquad \frac{dy}{dt} = -x$$

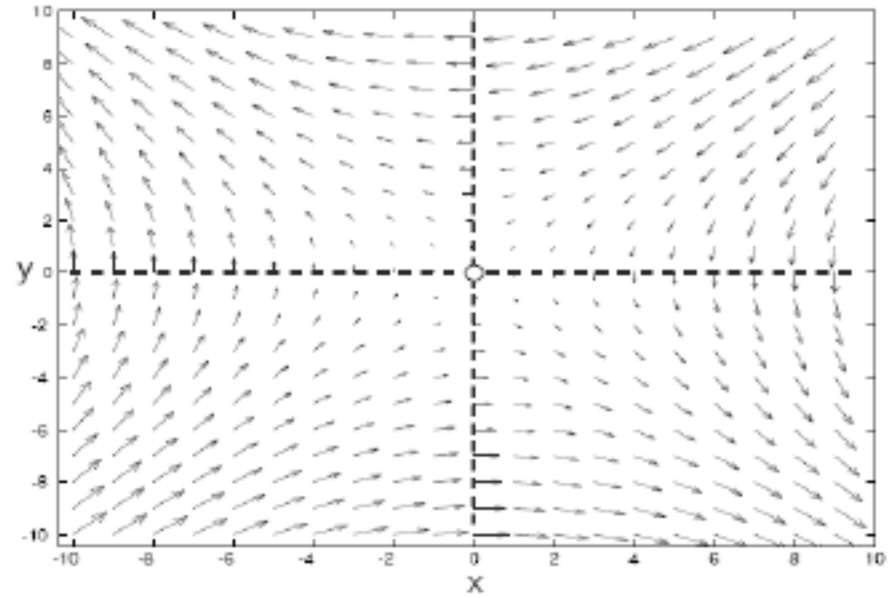

Two-dimensional dynamical systems

$$\frac{dx}{dt} = -y, \qquad \frac{dy}{dt} = -x$$

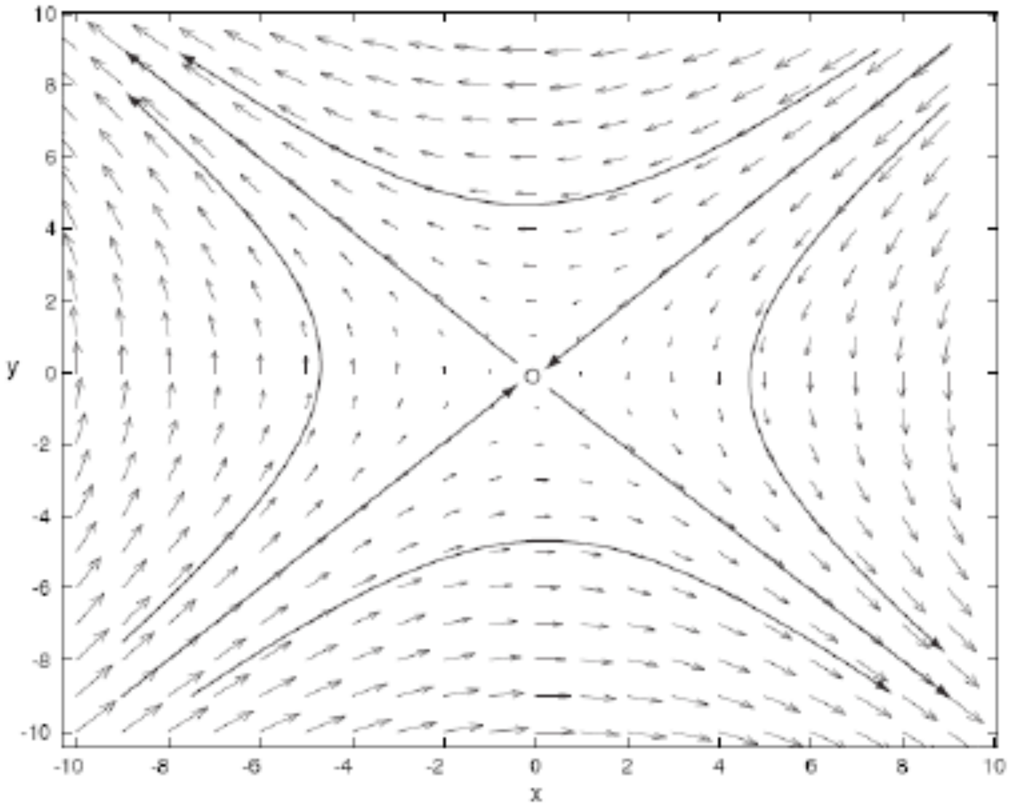

Solutions are trajectories tangent to the vector field

Two-dimensional dynamical systems

$$\frac{dx}{dt} = f(x,y), \qquad \frac{dy}{dt} = g(x,y)$$

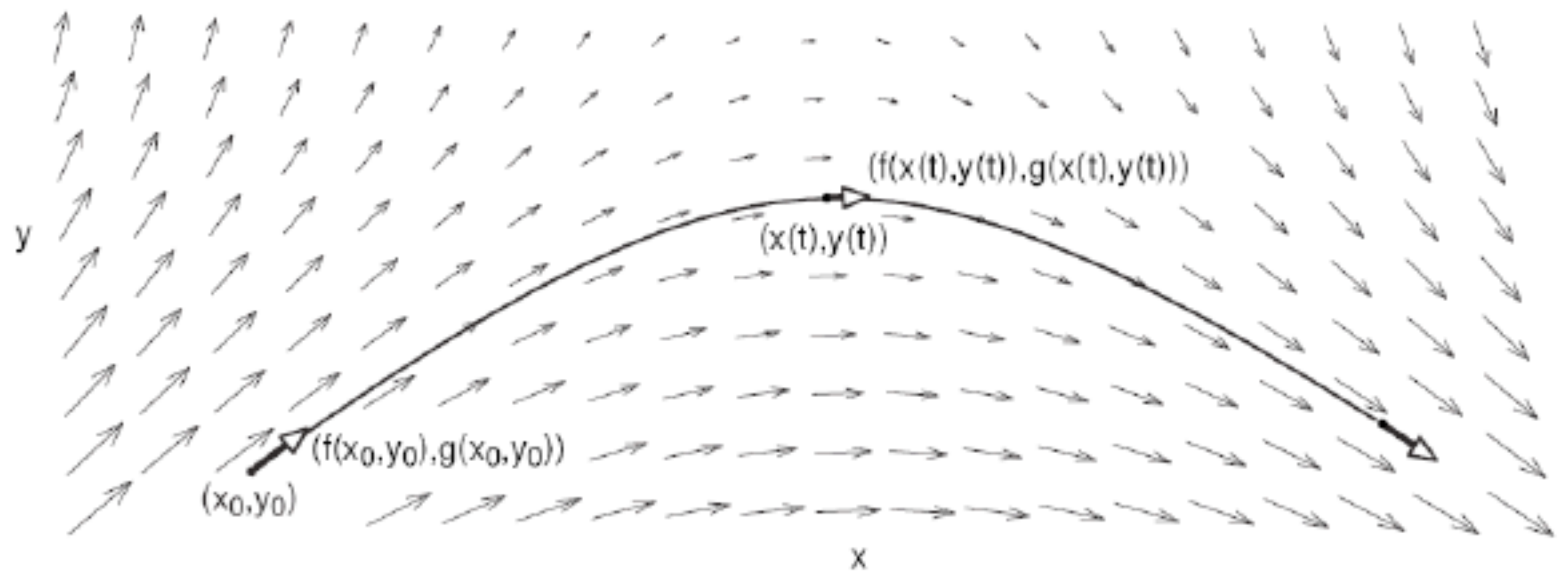

Solutions are trajectories tangent to the vector field

Two-dimensional dynamical systems

Limit cycles

$$\frac{dx}{dt} = f(x, y) \qquad \frac{dy}{dt} = g(x, y)$$

$$x(t) = x(t+T) \qquad y(t) = y(t+T)$$

- The minimal value of T for which the equality holds is called the period

Two-dimensional dynamical systems

Limit cycles

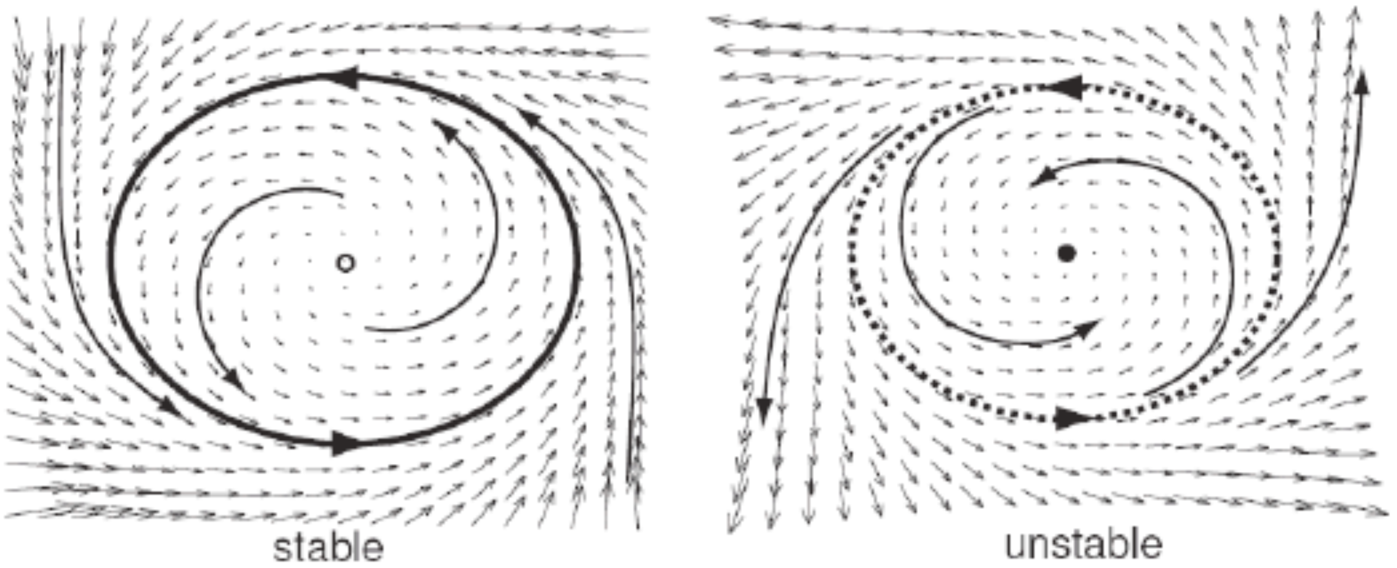

- The minimal value of T for which the equality holds is called the period

Two-dimensional neural models

- $I_{na,p} + I_K$ model

$$C\frac{dV}{dt} = - G_{Na}\, m_{\infty}(V)\,(V - E_{Na}) - G_K\, n\,(V - E_K) - G_L\,(V - E_L) + I$$

$$\frac{dn}{dt} = \frac{n_{\infty}(V) - n}{\tau_n(V)}$$

Two-dimensional neural models

- $I_{na,p} + I_K$ model

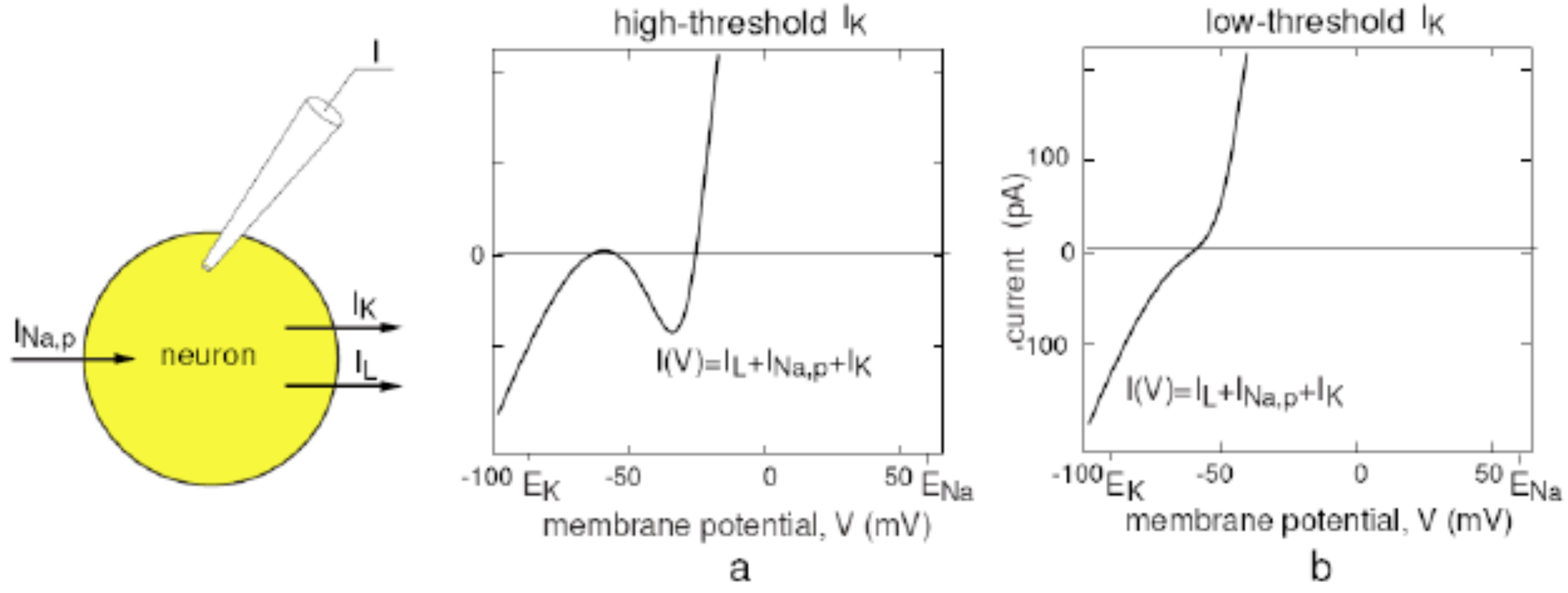

Figure 4.1: The $I_{Na,p}$+I_K-model (4.1, 4.2). Parameters in (a): $C = 1$, $I = 0$, $E_L = -80$ mV, $g_L = 8$, $g_{Na} = 20$, $g_K = 10$, $m_\infty(V)$ has $V_{1/2} = -20$ and $k = 15$, $n_\infty(V)$ has $V_{1/2} = -25$ and $k = 5$, and $\tau(V) = 1$, $E_{Na} = 60$ mV and $E_K = -90$ mV. Parameters in (b) as in (a) except $E_L = -78$ mV and $n_\infty(V)$ has $V_{1/2} = -45$; see Sect. 2.3.5.

Two-dimensional neural models

- Nullclines

$$n = \frac{I - G_L\ (V - E_L) - G_{Na} m_\infty(V)\ (V - E_{Na})}{G_K (V - E_K)}$$

$$n = n_\infty(V)$$

Two-dimensional neural models

- Phase-plane

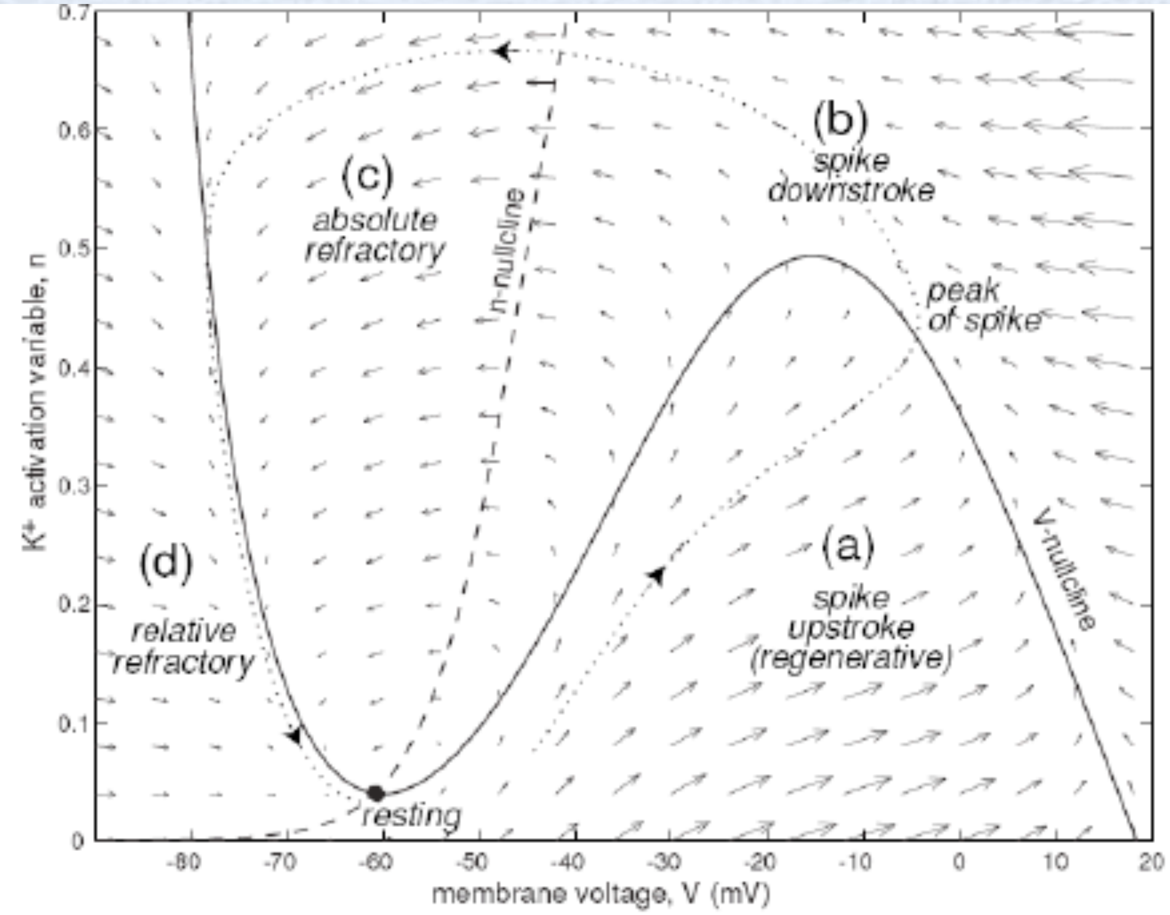

Figure 4.4: Nullclines of the $I_{\mathrm{Na,p}}+I_{\mathrm{K}}$-model (4.1, 4.2) with low-threshold K^+ current in Fig. 4.1b. (The vector field is slightly distorted for the sake of clarity of illustration).

Two-dimensional neural models

- Phase-plane

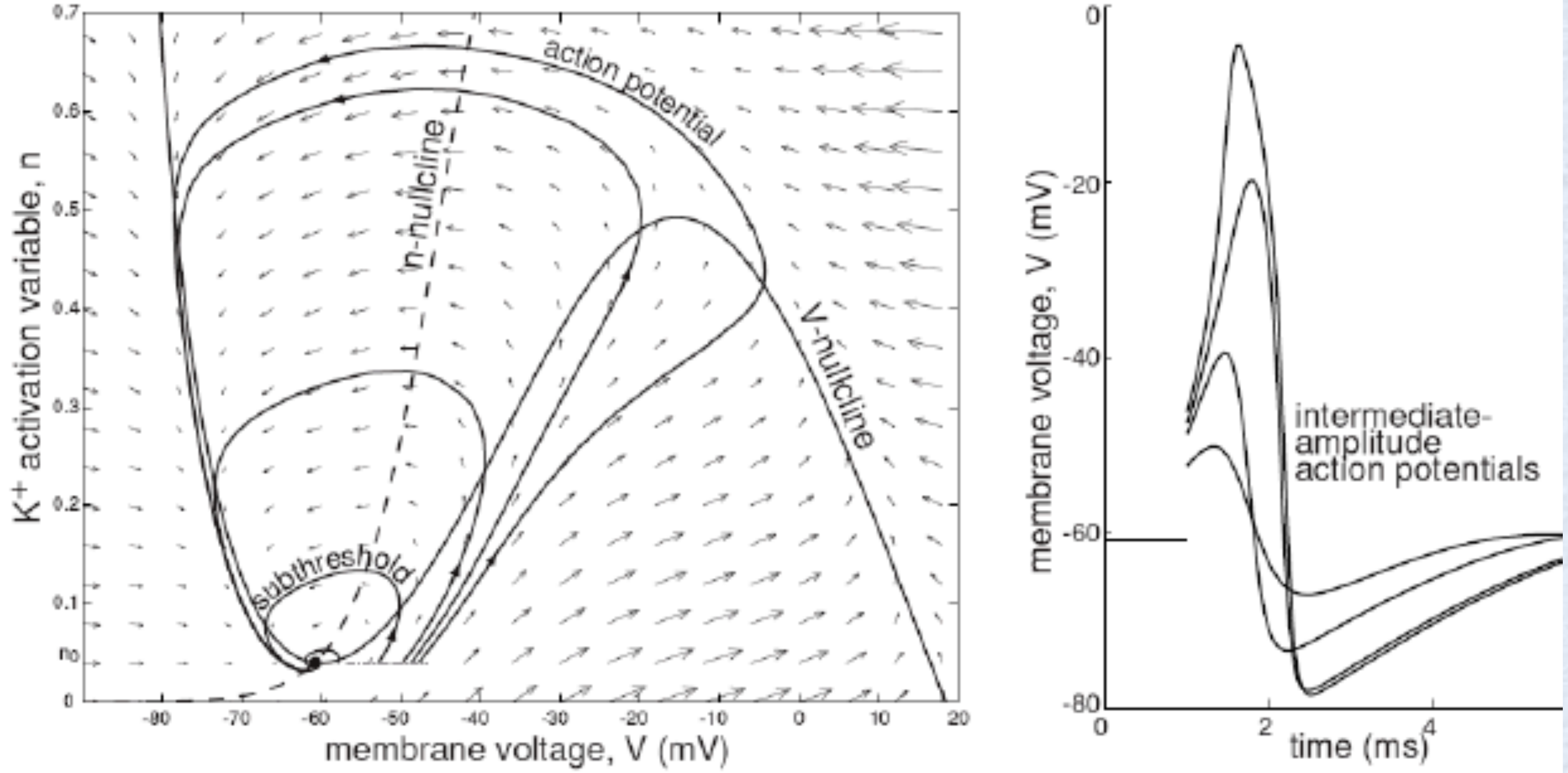

Failure to generate all-or-none action potentials in the $I_{Na,p}+I_K$-model

Two-dimensional neural models

- Phase-plane

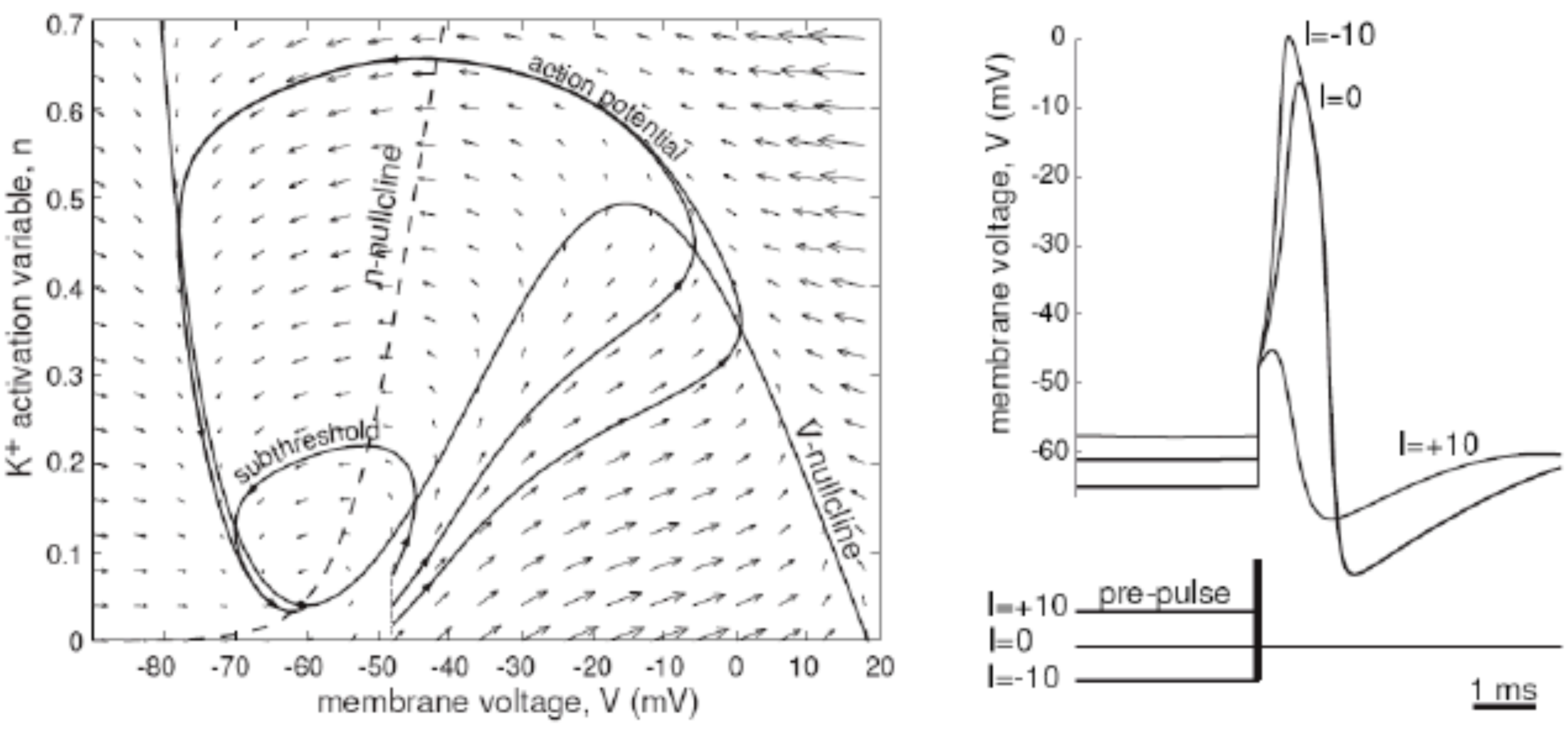

Failure to have a fixed value of threshold voltage in the $I_{\mathrm{Na,p}}+I_{\mathrm{K}}$-model

Two-dimensional neural models

- Limit cycle in the $I_{na,p} + I_K$ model with low-threshold K^+ and I = 40

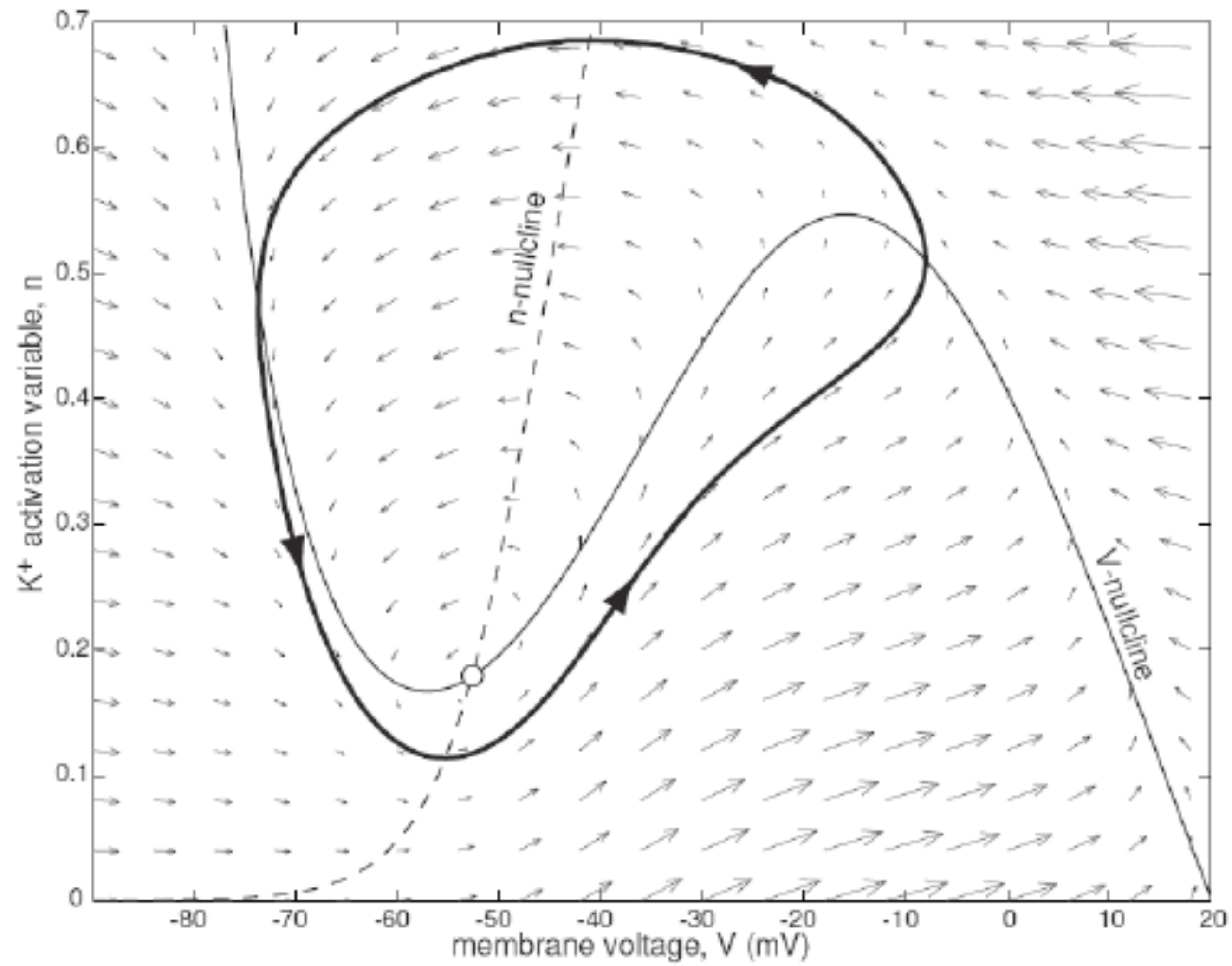

Two-dimensional neural models

- Limit cycle in the $I_{na,p}$ + I_K model with low-threshold K^+ and $I = 40$

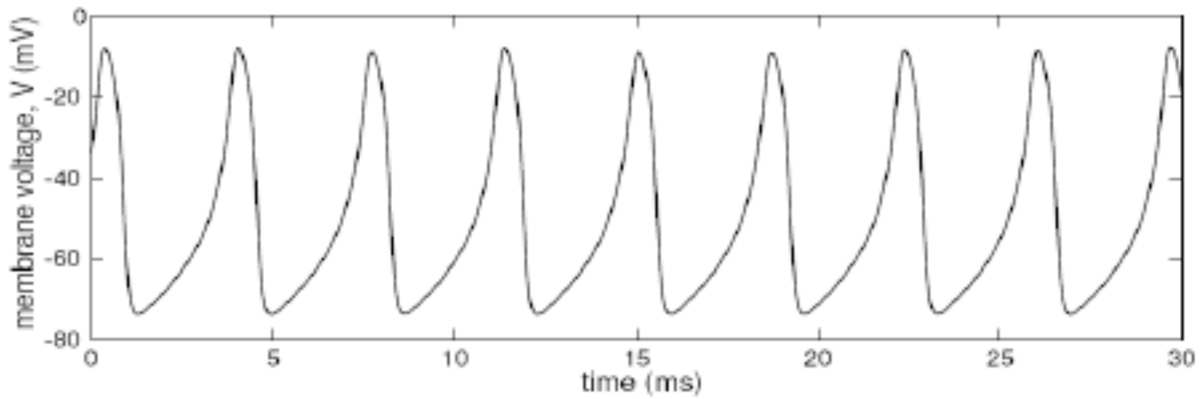

Two-dimensional neural models

- Limit cycle in the $I_{na,p} + I_K$ model with low-threshold K^+ and I = 40

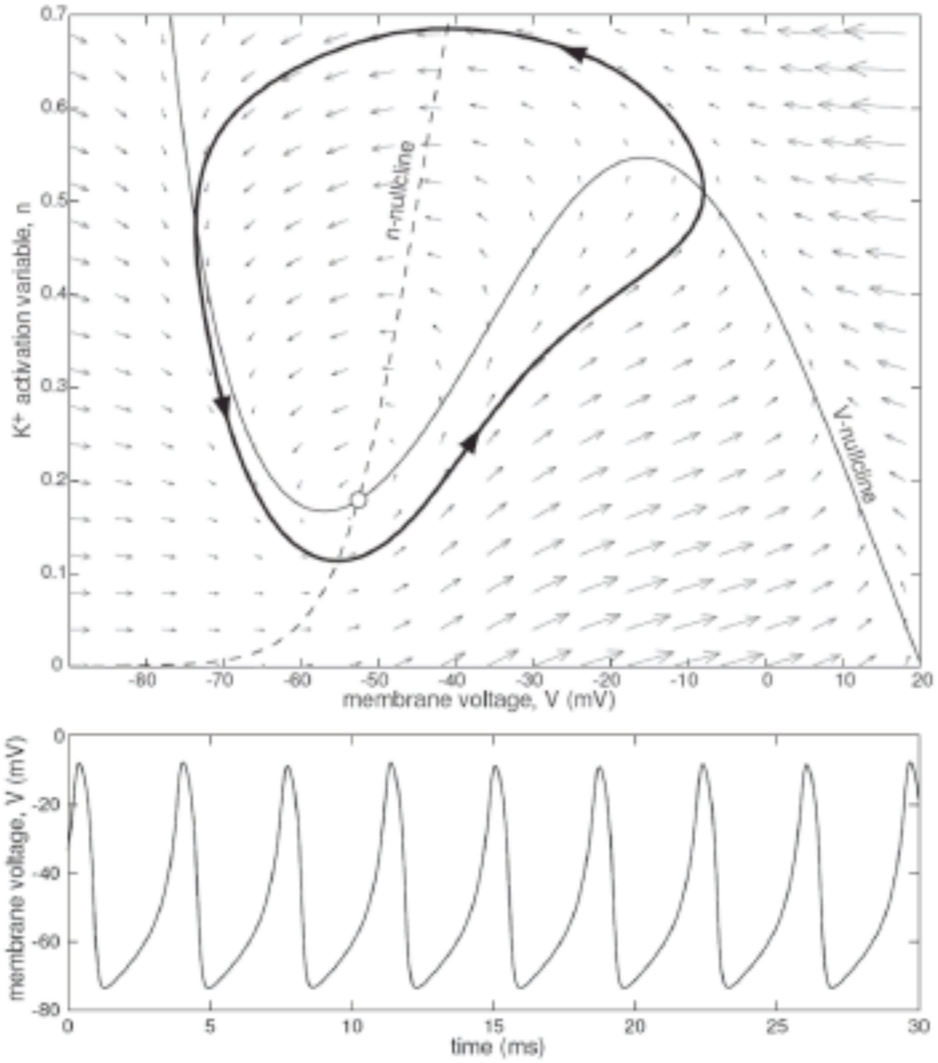

Two-dimensional neural models

- Limit cycles corresponding to tonic spiking of three types of neurons recorded *in vitro*

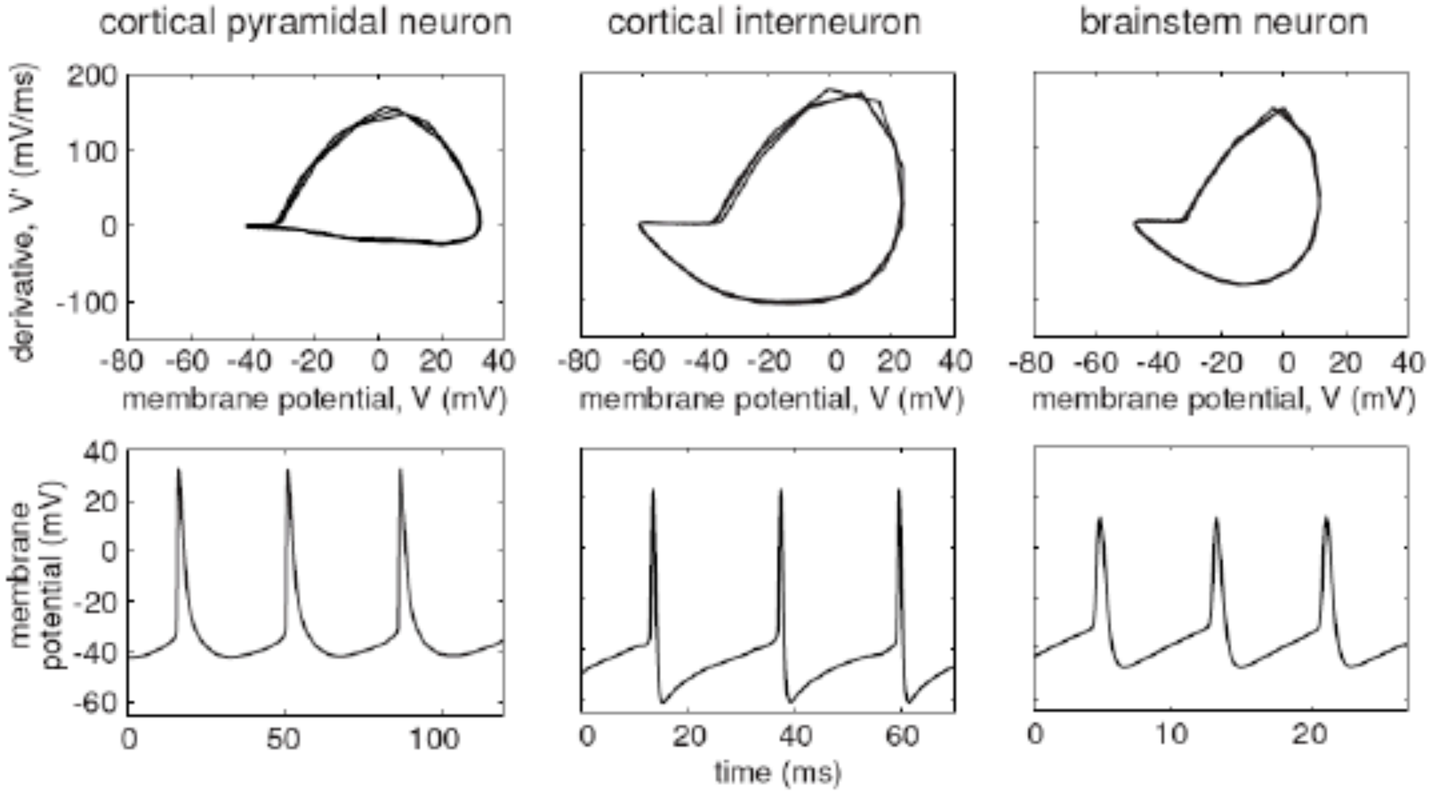

Two-dimensional neural models

- Relaxation oscillators

$$\frac{dx}{dt} = f(x, y)$$

$$\frac{dy}{dt} = \mu\, g(x, y)$$

$0 < \mu \ll 1$

Two-dimensional neural models

- Van de Pol model

$$\frac{dx}{dt} = x - x^3/3 - y \qquad \frac{dy}{dt} = \mu x \qquad \mu = 0.01$$

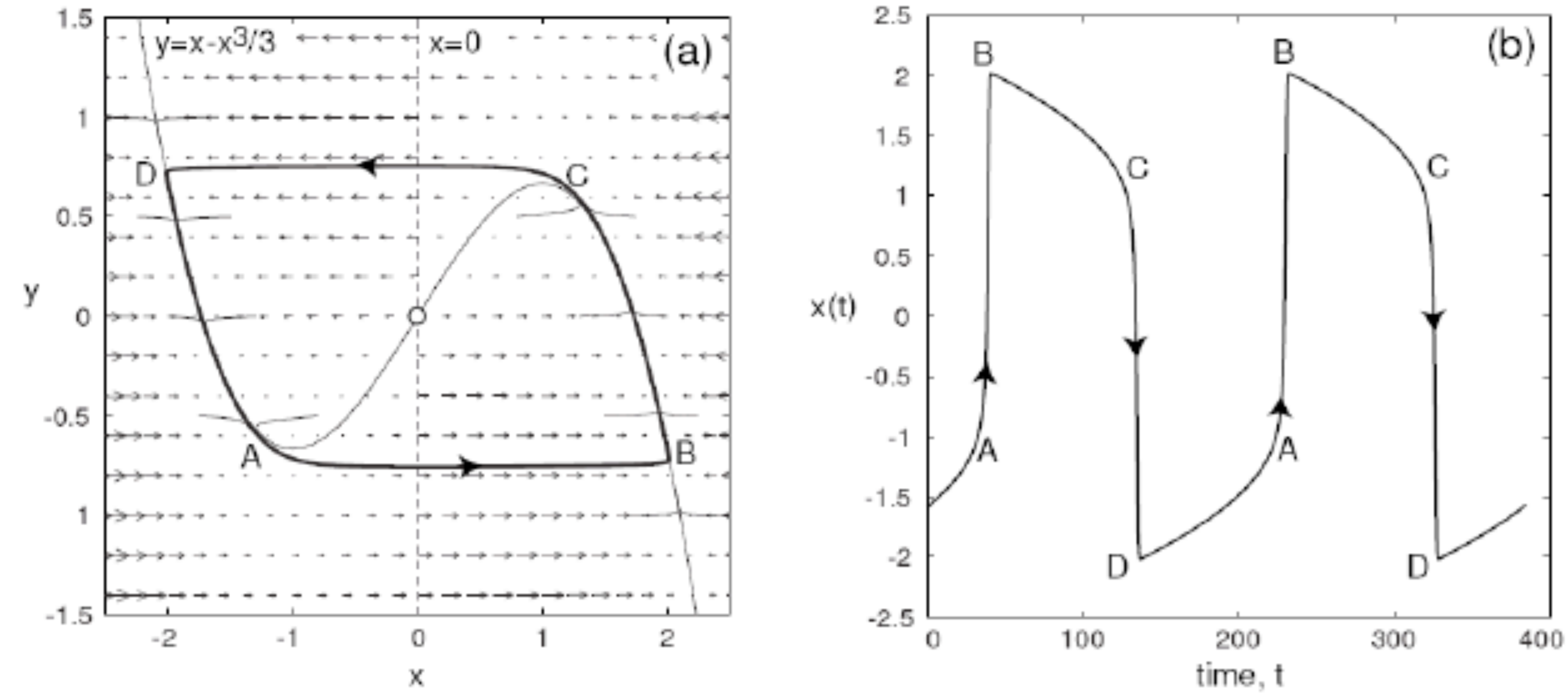

Two-dimensional neural models

- Equilibria

$$\frac{dx}{dt} = f(x, y) \qquad \frac{dy}{dt} = g(x, y)$$

$$f(x_0, y_0) = 0 \qquad g(x_0, y_0) = 0$$

Two-dimensional neural models

- Neutrally stable equilibria

$$\frac{dx}{dt} = f(x, y) \qquad \frac{dy}{dt} = g(x, y)$$

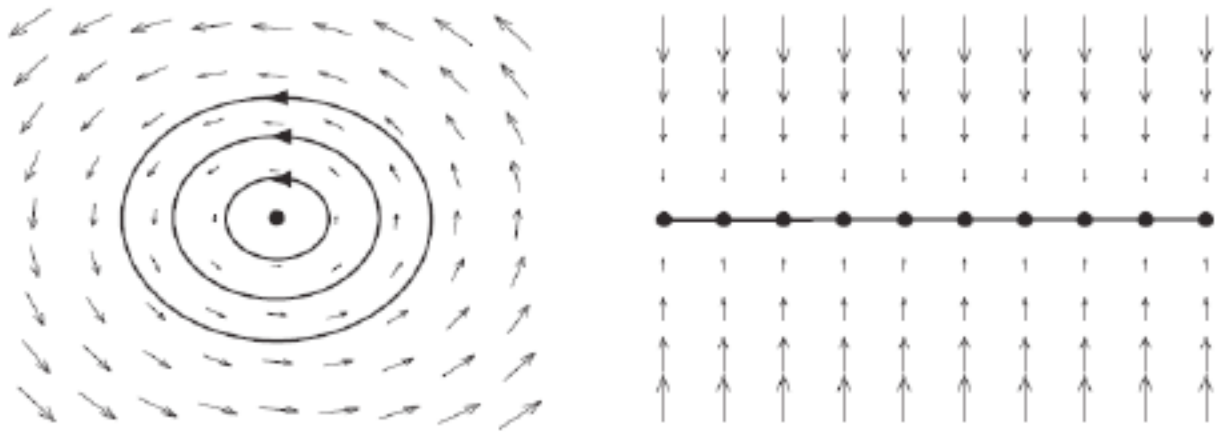

Two-dimensional neural models

- Unstable equilibria

$$\frac{dx}{dt} = f(x, y) \qquad \frac{dy}{dt} = g(x, y)$$

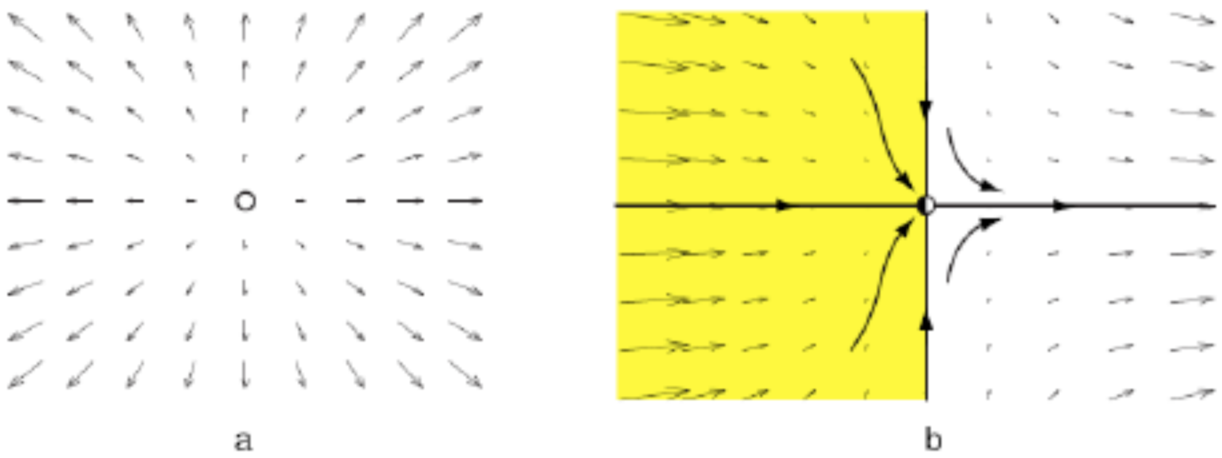

Two-dimensional neural models

- Stable equilibria

$$\frac{dx}{dt} = f(x, y) \qquad \frac{dy}{dt} = g(x, y)$$

- Asymptotically stable
- Exponentially stable
- Neutrally stable

Two-dimensional neural models

- Local linear analysis

$$\frac{dx}{dt} = f(x, y) \qquad \frac{dy}{dt} = g(x, y)$$

- Taylor expansion

$$f(x, y) = a(x - x_0) + b(y - y_0) + h.o.t.$$
$$g(x, y) = c(x - x_0) + d(y - y_0) + h.o.t.$$

$$a := f_x(x_0, y_0) \qquad b := f_y(x_0, y_0)$$
$$c := g_x(x_0, y_0) \qquad d := g_y(x_0, y_0)$$

Two-dimensional neural models

- Local linear analysis

$$v := x - x_0 \qquad w := y - y_0$$

$$\begin{pmatrix} v' \\ w' \end{pmatrix} = \begin{pmatrix} a & b \\ c & d \end{pmatrix} \begin{pmatrix} v \\ w \end{pmatrix} = L \begin{pmatrix} v \\ w \end{pmatrix}$$

L : Jacobian Matrix

$$\begin{pmatrix} v \\ w \end{pmatrix} = c_k \begin{pmatrix} u_v \\ u_w \end{pmatrix} e^{\lambda t} \qquad k = 1, 2$$

Two-dimensional neural models

- Eigenvalues and eigenvectors

$$L\begin{pmatrix} u_v \\ u_w \end{pmatrix} = \begin{pmatrix} a & b \\ c & d \end{pmatrix}\begin{pmatrix} u_v \\ u_w \end{pmatrix} = \lambda\begin{pmatrix} u_v \\ u_w \end{pmatrix}$$

$$(L - \lambda I)\begin{pmatrix} u_v \\ u_w \end{pmatrix} = \begin{pmatrix} 0 \\ 0 \end{pmatrix}$$

$$\det(L - \lambda I) = \begin{vmatrix} a - \lambda & b \\ c & d - \lambda \end{vmatrix} = 0$$

Two-dimensional neural models

- Eigenvalues and eigenvectors

$$\lambda^2 - (a + d)\lambda + (ad - bc) = 0$$

$$\lambda^2 - \tau\ \lambda + \Delta = 0$$

$$\tau = a + d \qquad \Delta = ad - bc$$

Two-dimensional neural models

- Eigenvalues and eigenvectors

$$\lambda_1 = \frac{\tau + \sqrt{\tau^2 - 4\Delta}}{2} \qquad \lambda_2 = \frac{\tau - \sqrt{\tau^2 - 4\Delta}}{2}$$

$$\begin{pmatrix} v \\ w \end{pmatrix} = c_1 \begin{pmatrix} u_{v,1} \\ u_{w,1} \end{pmatrix} e^{\lambda_1 t} + c_2 \begin{pmatrix} u_{v,2} \\ u_{w,2} \end{pmatrix} e^{\lambda_2 t}$$

Two-dimensional neural models

- $$\lambda_{1,2} = \frac{\tau \pm \sqrt{\tau^2 - 4\Delta}}{2}$$ $$\begin{pmatrix} v \\ w \end{pmatrix} = c_1 \begin{pmatrix} u_{v,1} \\ u_{w,1} \end{pmatrix} e^{\lambda_1 t} + c_2 \begin{pmatrix} u_{v,2} \\ u_{w,2} \end{pmatrix} e^{\lambda_2 t}$$

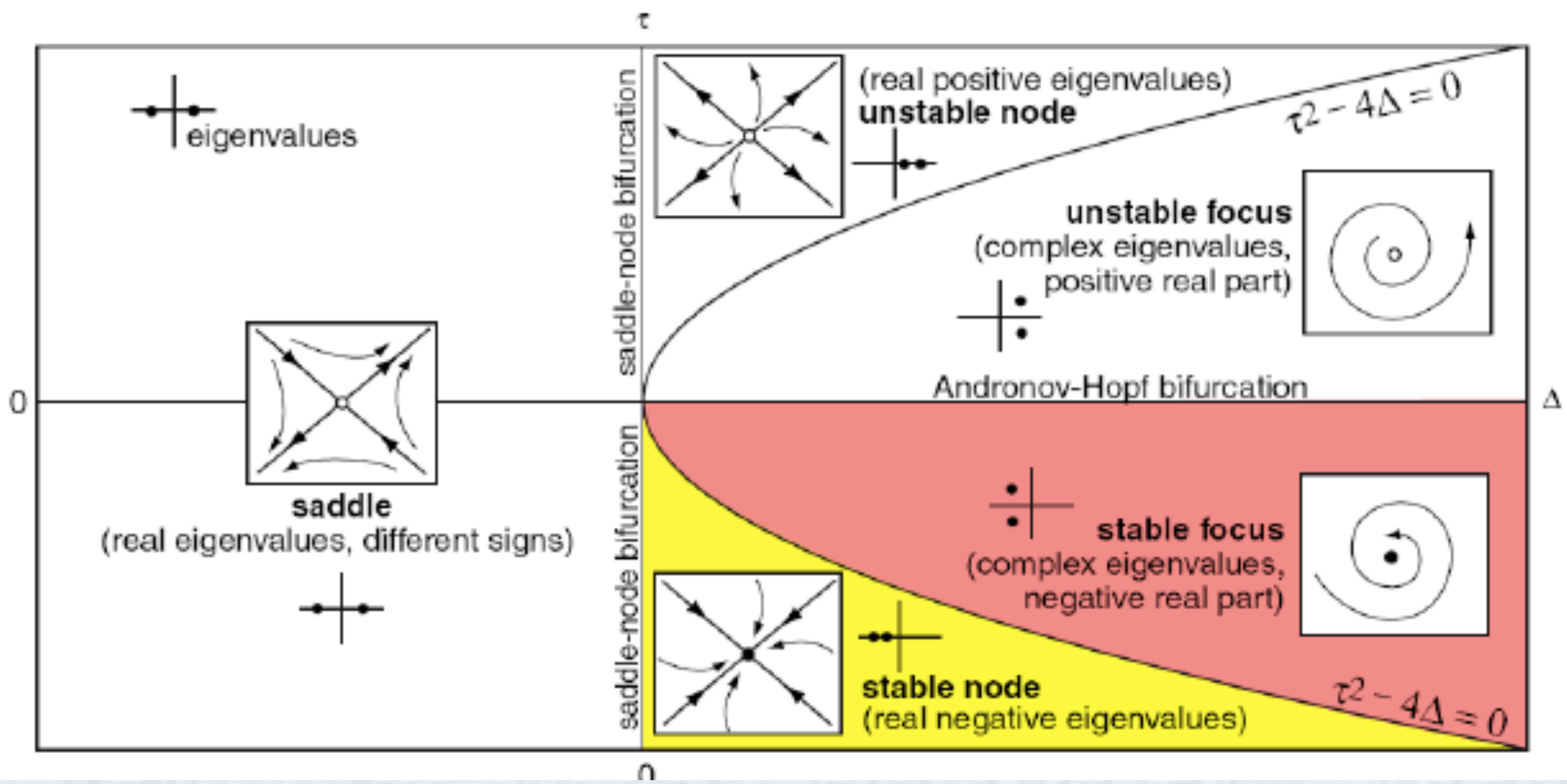

Two-dimensional neural models

- $\lambda_{1,2} = \dfrac{\tau \pm \sqrt{\tau^2 - 4\Delta}}{2}$

$$\begin{pmatrix} v \\ w \end{pmatrix} = c_1 \begin{pmatrix} u_{v,1} \\ u_{w,1} \end{pmatrix} e^{\lambda_1 t} + c_2 \begin{pmatrix} u_{v,2} \\ u_{w,2} \end{pmatrix} e^{\lambda_2 t}$$

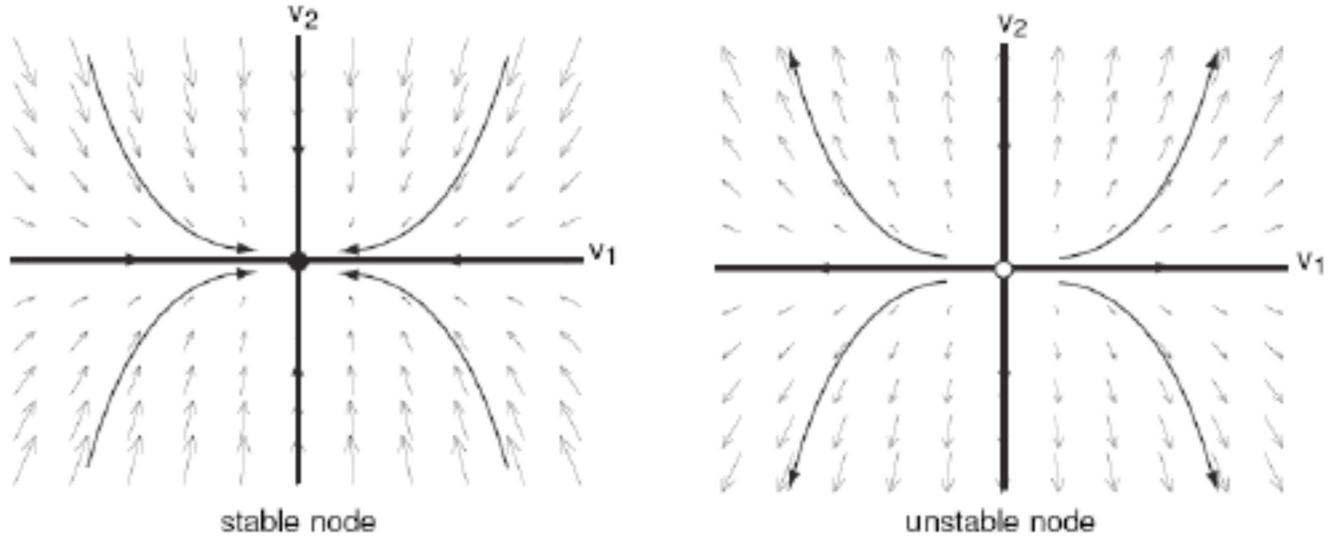

Figure 4.16: Node equilibrium occurs when both eigenvalues are real and have the same sign, e.g., $\lambda_1 = -1$ and $\lambda_2 = -3$ (stable) or $\lambda_1 = +1$ and $\lambda_2 = +3$ (unstable). Most trajectories converge to or diverge from the node along the eigenvector v_1 corresponding to the eigenvalue having the smallest absolute value.

Two-dimensional neural models

- $\lambda_{1,2} = \frac{\tau \pm \sqrt{\tau^2 - 4\Delta}}{2}$ $\quad \begin{pmatrix} v \\ w \end{pmatrix} = c_1 \begin{pmatrix} u_{v,1} \\ u_{w,1} \end{pmatrix} e^{\lambda_1 t} + c_2 \begin{pmatrix} u_{v,2} \\ u_{w,2} \end{pmatrix} e^{\lambda_2 t}$

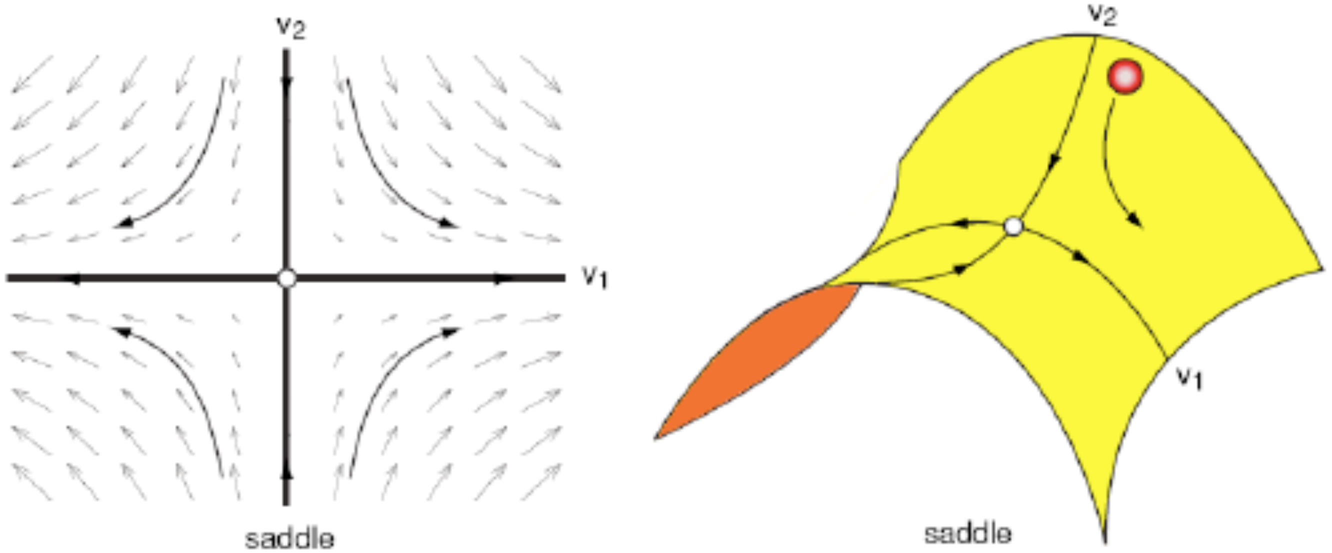

Figure 4.17: Saddle equilibrium occurs when two real eigenvalues have opposite signs, e.g., $\lambda_1 = +1$ and $\lambda_2 = -1$. Most trajectories diverge from the equilibrium along the eigenvector corresponding to the positive eigenvalue (in this case v_1).

Two-dimensional neural models

- $\lambda_{1,2} = \dfrac{\tau \pm \sqrt{\tau^2 - 4\Delta}}{2}$ $\qquad \begin{pmatrix} v \\ w \end{pmatrix} = c_1 \begin{pmatrix} u_{v,1} \\ u_{w,1} \end{pmatrix} e^{\lambda_1 t} + c_2 \begin{pmatrix} u_{v,2} \\ u_{w,2} \end{pmatrix} e^{\lambda_2 t}$

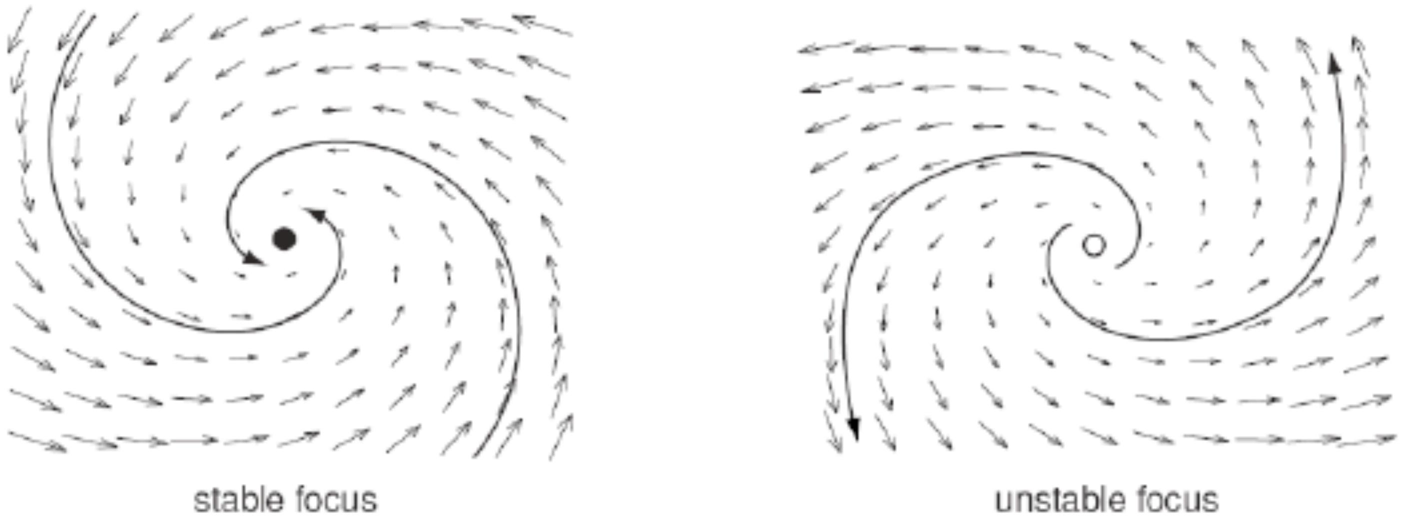

Figure 4.18: Focus equilibrium occurs when the eigenvalues are complex-conjugate, e.g., $\lambda = -3 \pm i$ (stable) or $\lambda = +3 \pm i$ (unstable). The imaginary part (here 1) determines the frequency of rotation around the focus.

Two-dimensional neural models

- Phase portrait of the $I_{na,p}$ + I_K model with high-threshold K^+ current

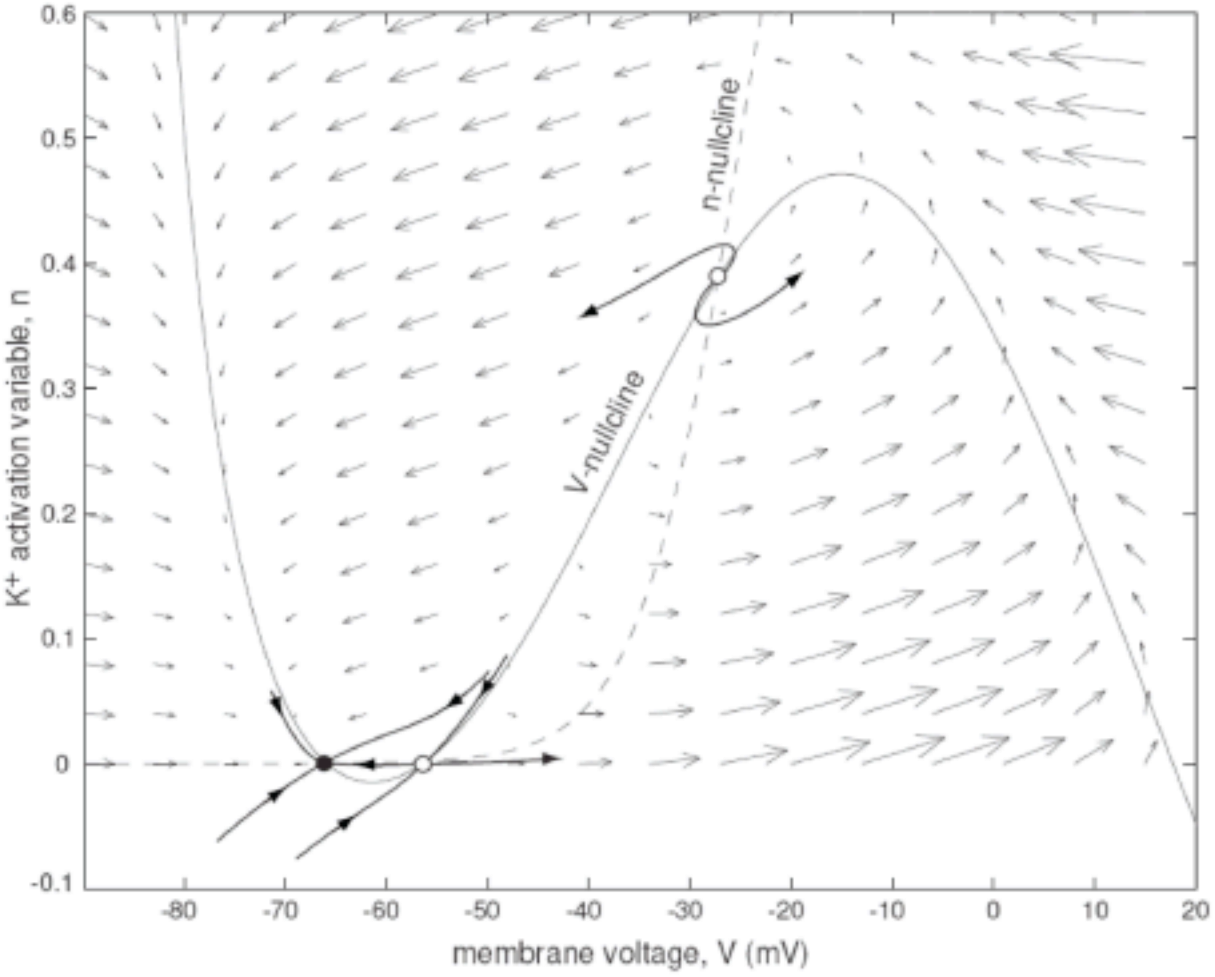

Two-dimensional neural models

- FitzHugh-Nagumo model

$$V' = V(a - V)(V - 1) - w + I$$
$$w' = bV - cw$$

- Nullclines

$$w = V(a - V)(V - 1) + I$$
$$w = \frac{b}{c}V$$

$$\tau = -a - c \qquad \Delta = ac + b$$

Two-dimensional neural models

❑ FitzHugh-Nagumo model

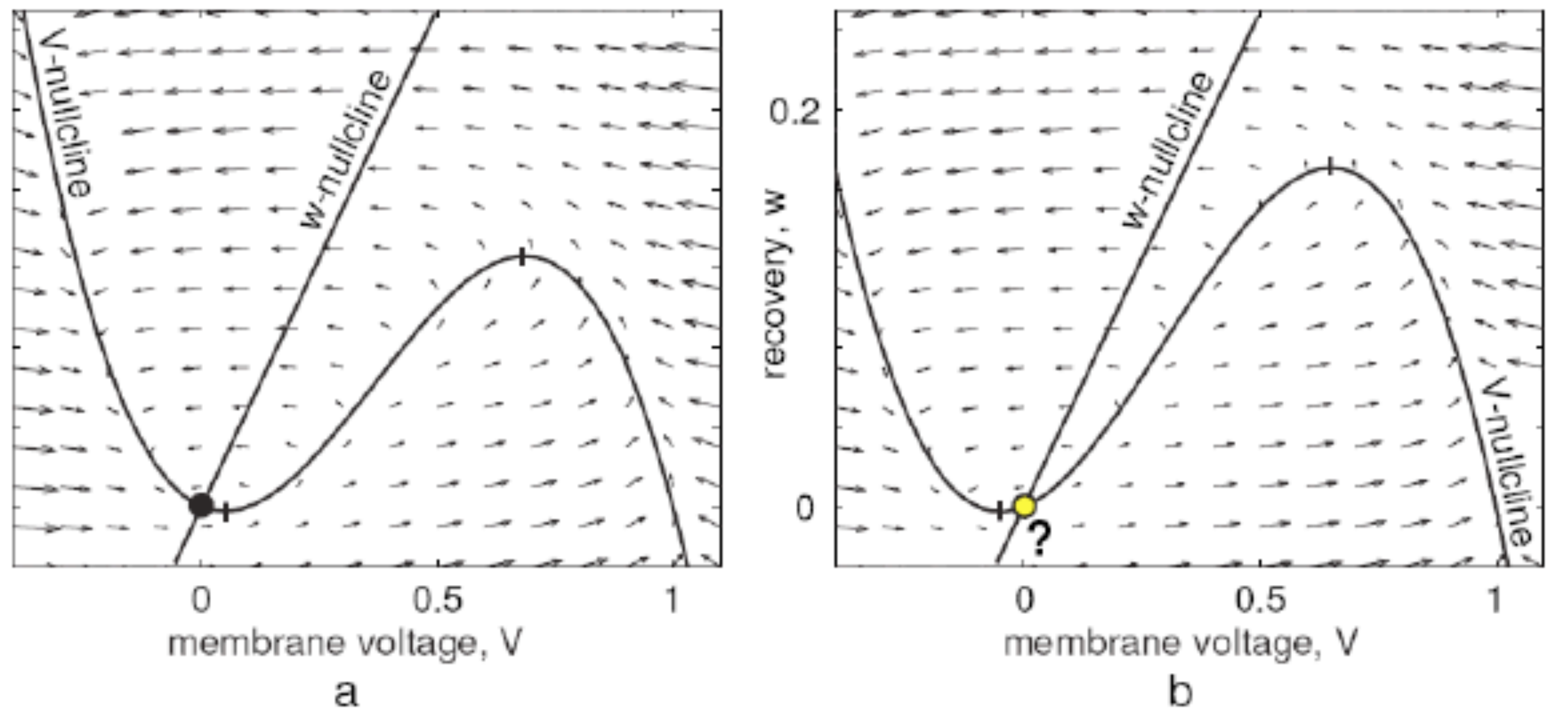

Figure 4.20: Nullclines in the FitzHugh-Nagumo model (4.11, 4.12). Parameters: $I = 0, b = 0.01, c = 0.02, a = 0.1$ (left) and $a = -0.1$ (right).

Two-dimensional neural models

❑ FitzHugh-Nagumo model

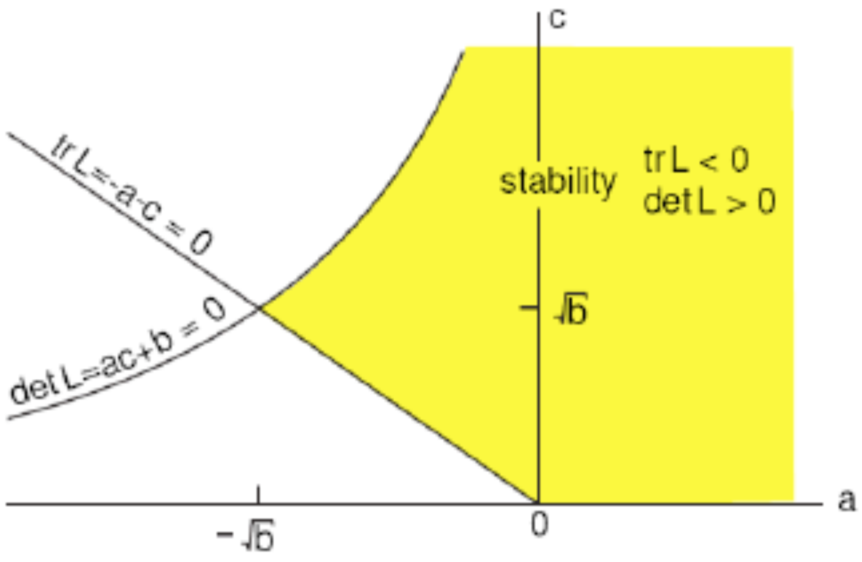

Figure 4.21: Stability diagram of the equilibrium (0, 0) in the FitzHugh-Nagumo model (4.11,4.12).

Two-dimensional neural models

- FitzHugh-Nagumo model

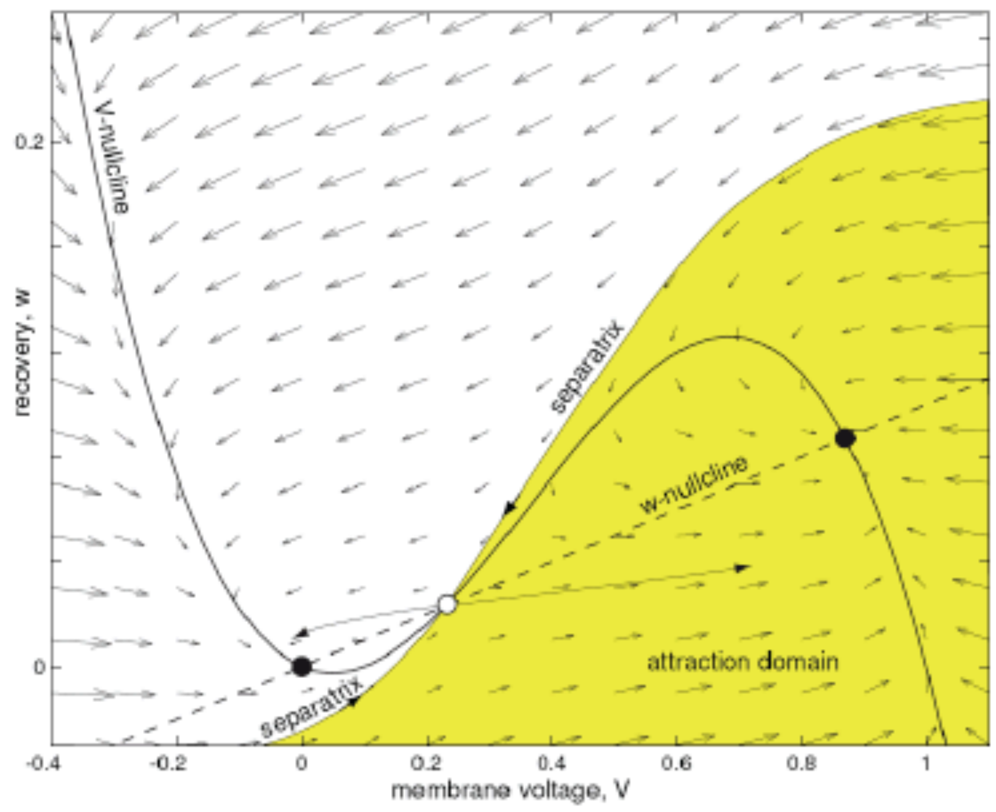

Figure 4.22: Bistability of two equilibrium attractors (black circles) in the FitzHugh-Nagumo model (4.11,4.12). The shaded area — attraction domain of the right equilibrium. Parameters: $I = 0$, $b = 0.01$, $a = c = 0.1$.

Two-dimensional neural models

- Bistability

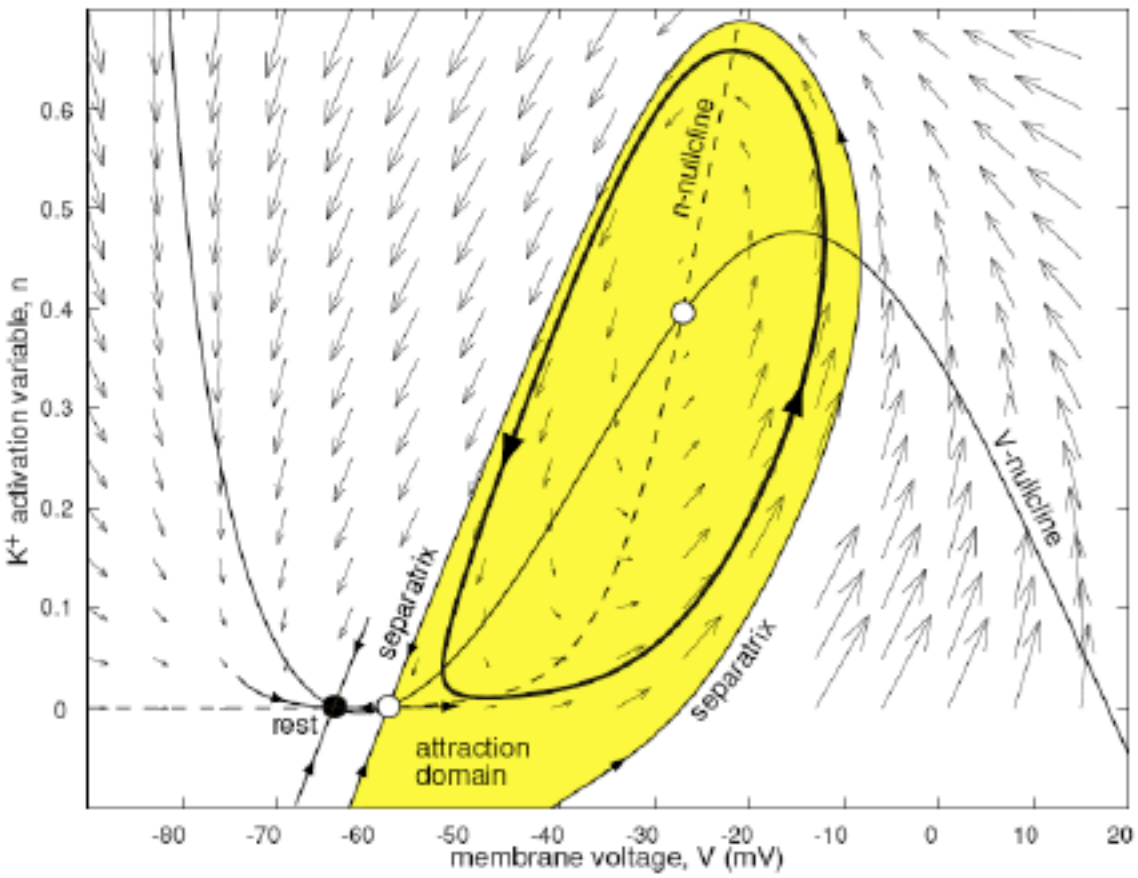

Figure 4.23: Bistability of rest and spiking states in the $I_{Na,p}+I_K$-model (4.1, 4.2) with high-threshold fast ($\tau(V) = 0.152$) K^+ current and $I = 3$. A brief strong pulse of current (arrow) brings the state vector of the system into the attraction domain of the stable limit cycle.

Two-dimensional neural models

Bistability

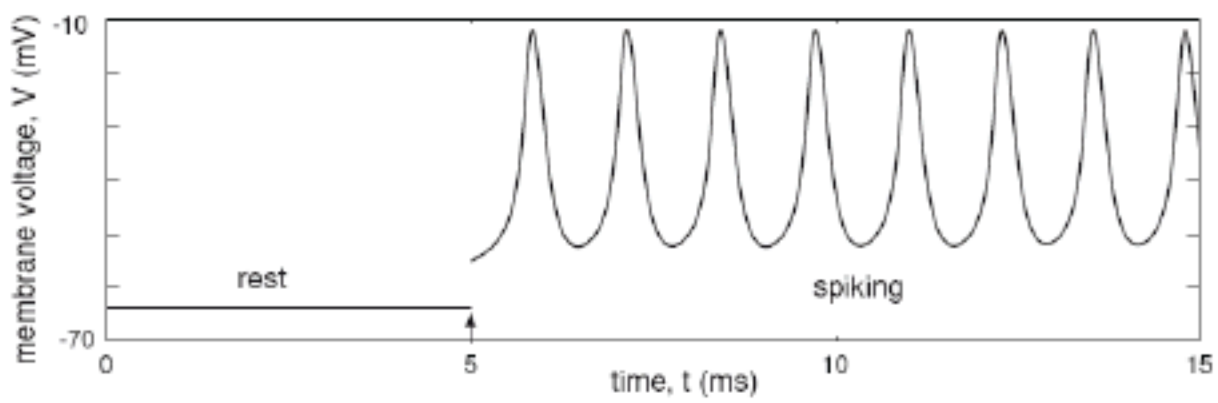

Figure 4.23: Bistability of rest and spiking states in the $I_{Na,p}+I_K$-model (4.1, 4.2) with high-threshold fast ($\tau(V) = 0.152$) K^+ current and $I = 3$. A brief strong pulse of current (arrow) brings the state vector of the system into the attraction domain of the stable limit cycle.

Two-dimensional neural models

- Stable and unstable manifolds

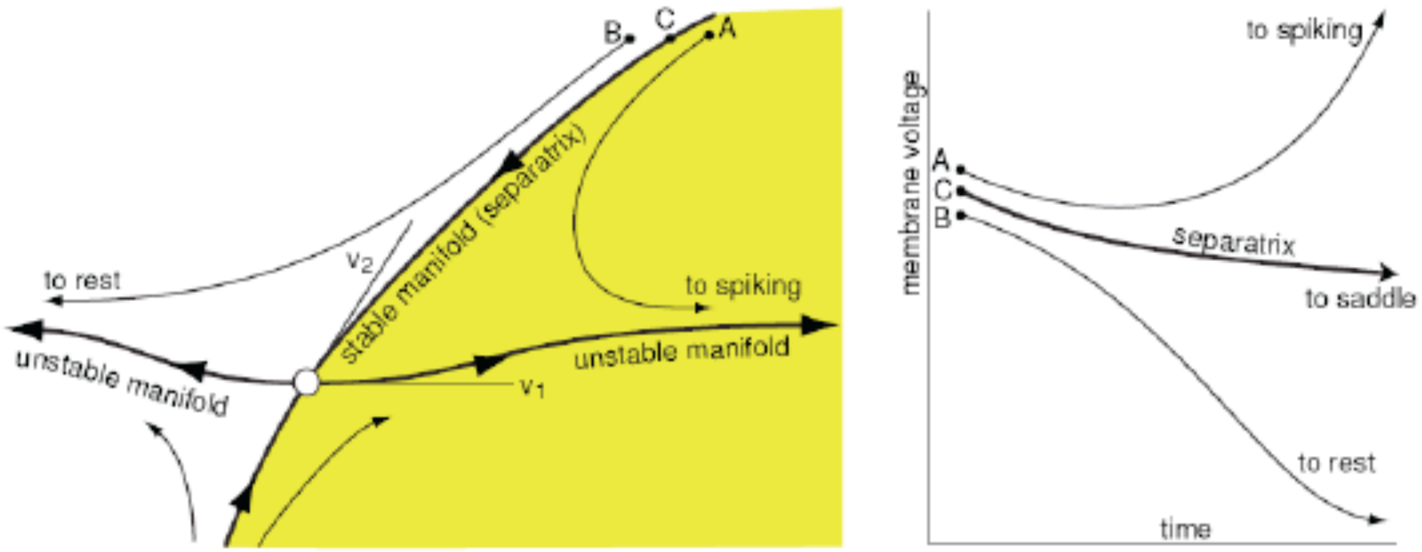

Figure 4.24: Stable and unstable manifolds to a saddle. The eigenvectors v_1 and v_2 correspond to positive and negative eigenvalues, respectively.

Two-dimensional neural models

- Homoclinic and heteroclinic trajectories

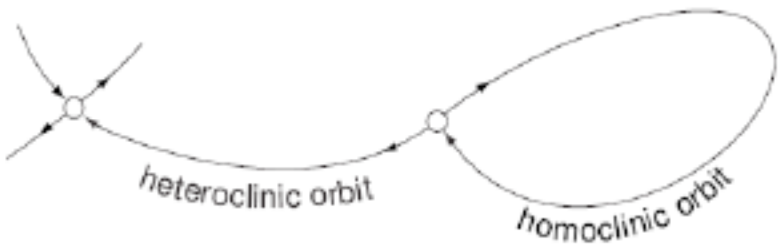

Figure 4.25: A heteroclinic orbit starts and ends at different equilibria. A homoclinic orbit starts and ends at the same equilibrium.

Two-dimensional neural models

- Homoclinic and heteroclinic trajectories

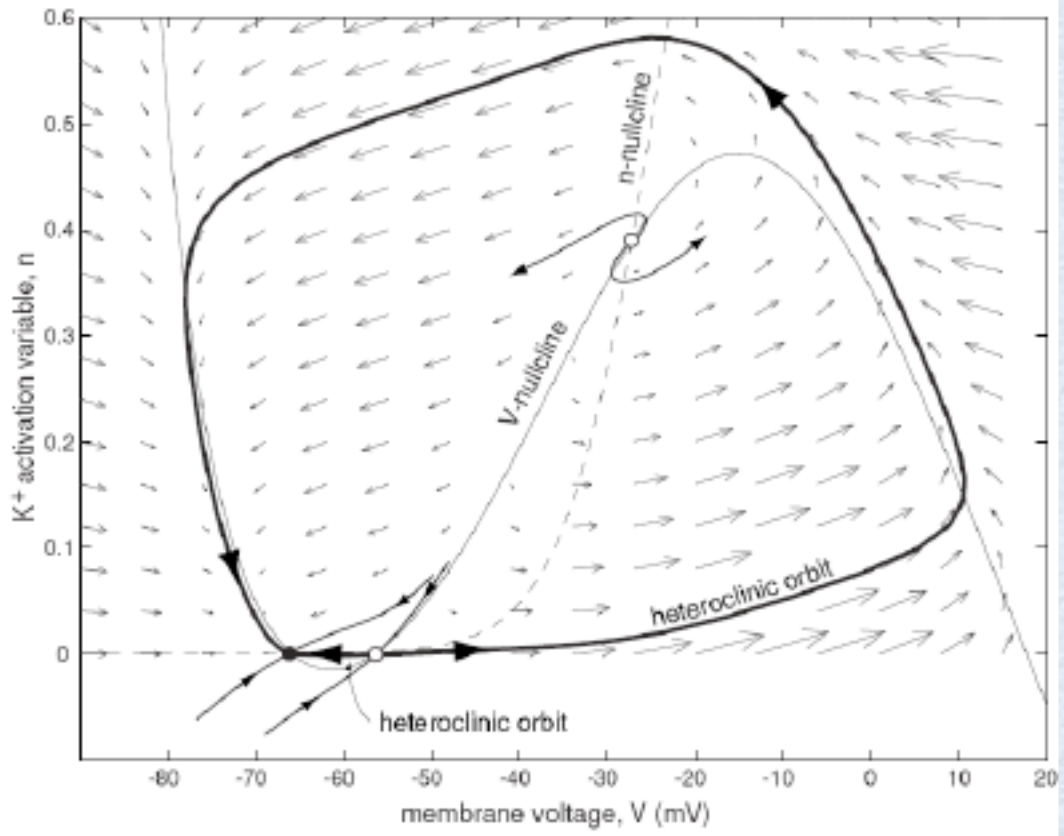

Figure 4.26: Two heteroclinic orbits (bold curves connecting stable and unstable equilibria) in the $I_{\mathrm{Na,p}}+I_{\mathrm{K}}$-model with high-threshold K^+ current.

Two-dimensional neural models

- Homoclinic and heteroclinic trajectories

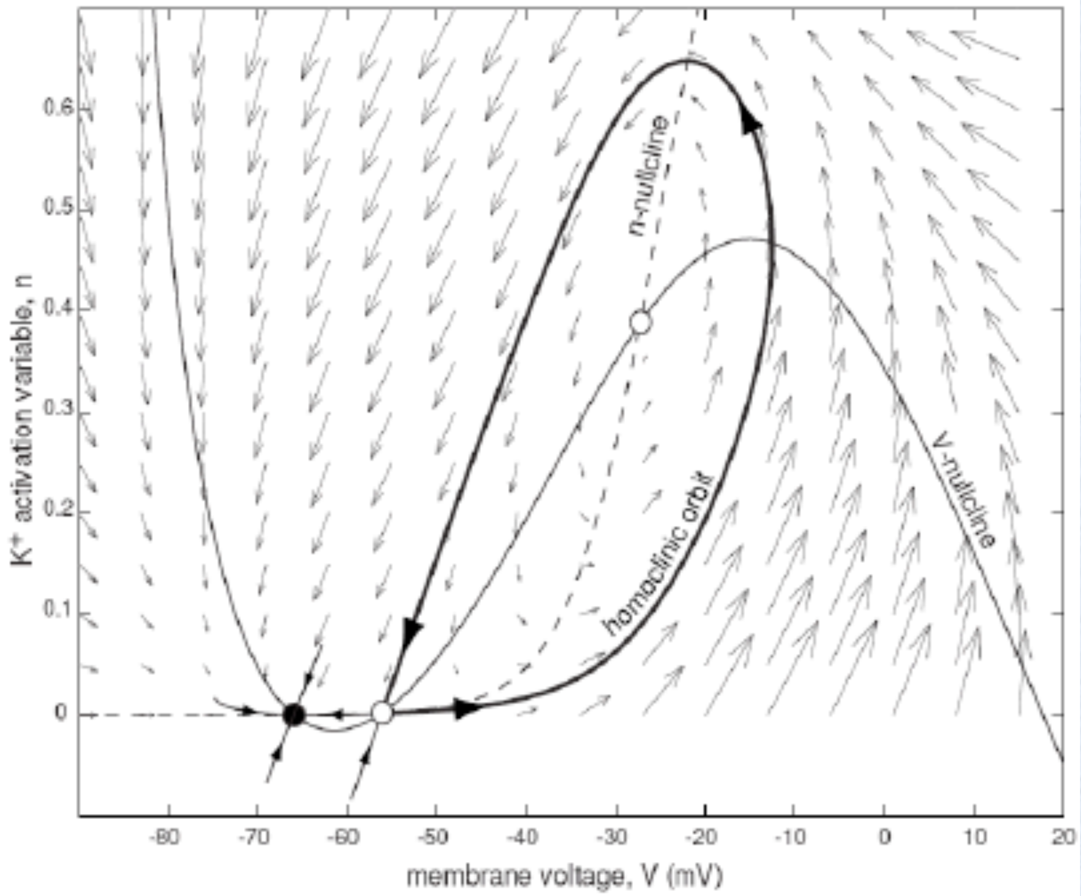

Figure 4.27: Homoclinic orbit (bold) in the $I_{Na,p}+I_K$-model with high-threshold fast ($\tau(V) = 0.152$) K^+ current.

Two-dimensional neural models

- Homoclinic and heteroclinic trajectories

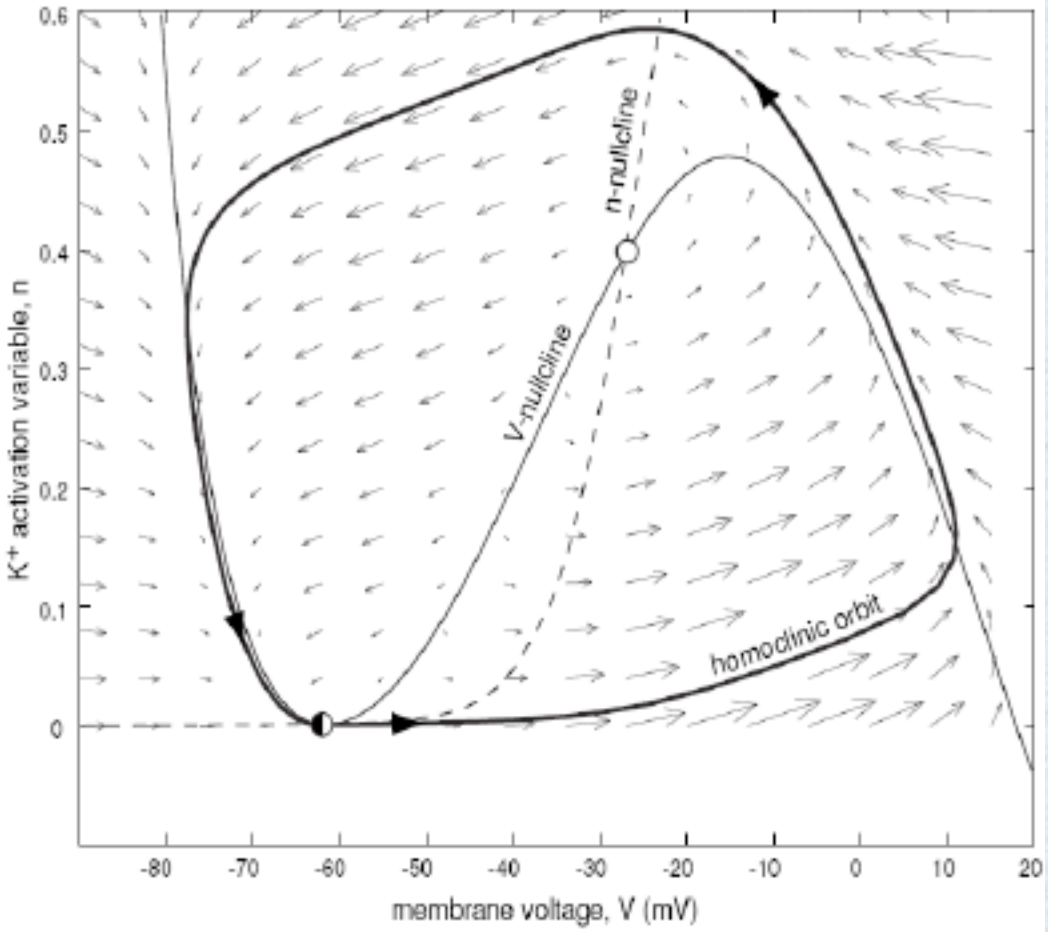

Figure 4.28: Homoclinic orbit (bold) to saddle-node equilibrium in the $I_{\mathrm{Na,p}}+I_{\mathrm{K}}$-model with high-threshold K^+ current and $I = 4.51$.

Two-dimensional neural models

- Saddle-node bifurcation

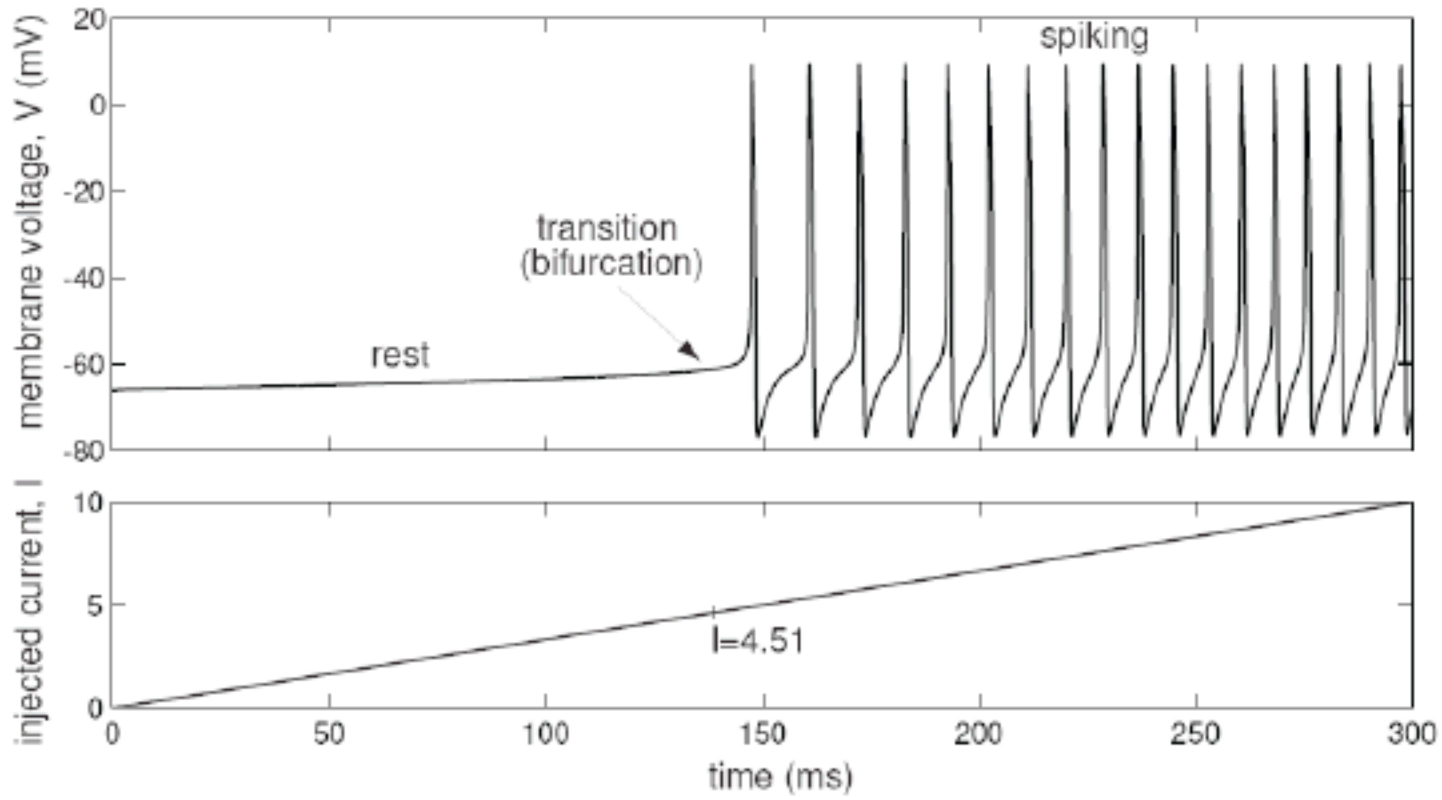

Transition from rest state to repetitive spiking in the $I_{Na,p}+I_K$-model

Two-dimensional neural models

- Limit cycle attractor

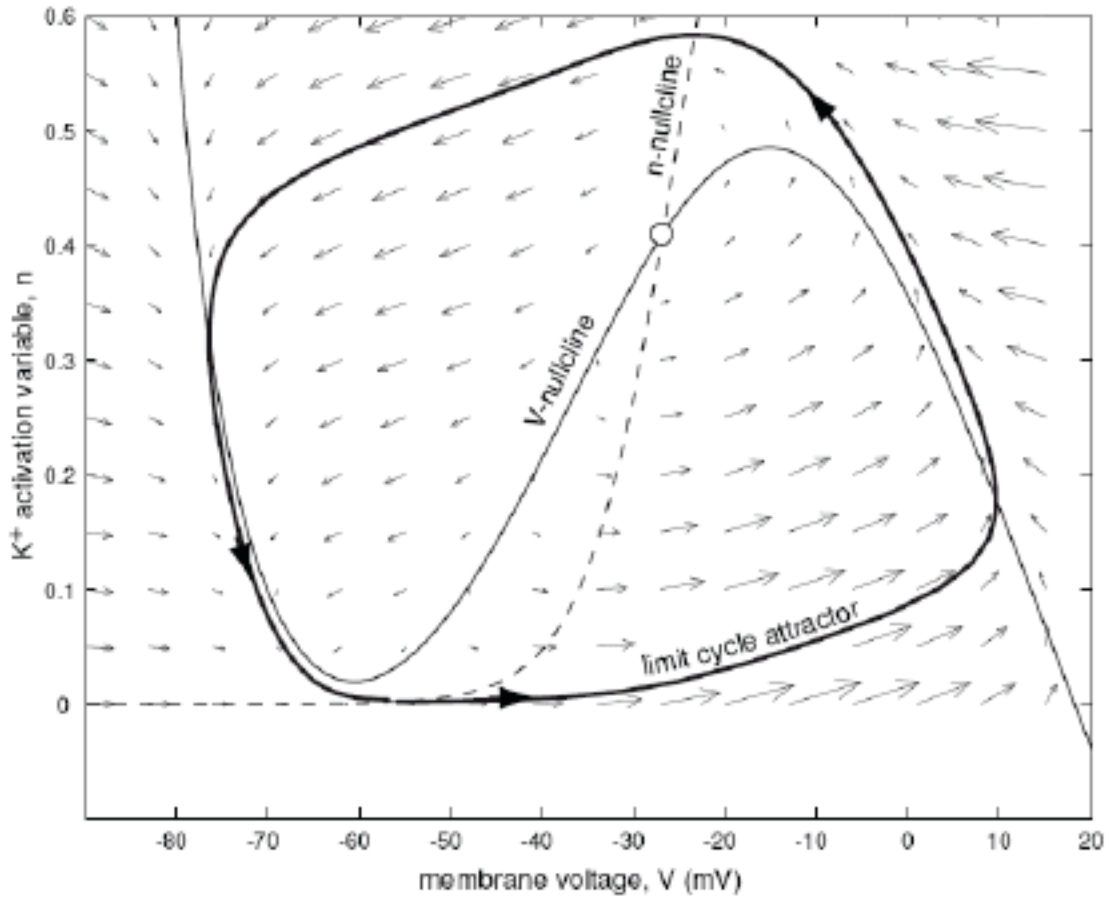

Limit cycle attractor (bold) in the $I_{\text{Na,p}}+I_{\text{K}}$-model when $I = 10$

Two-dimensional neural models

- Saddle-node bifurcation

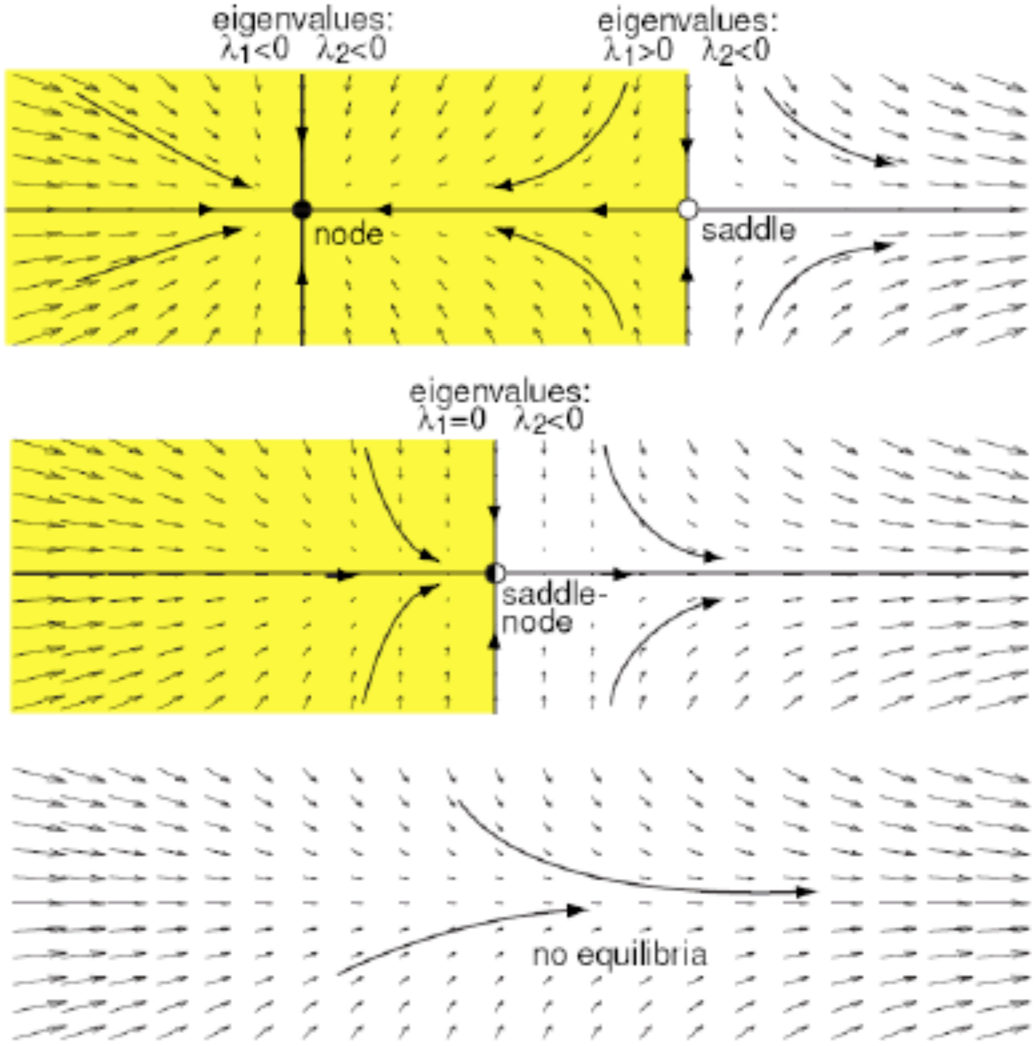

Two-dimensional neural models

- Saddle-node bifurcation in the $I_{na,p} + I_K$ model

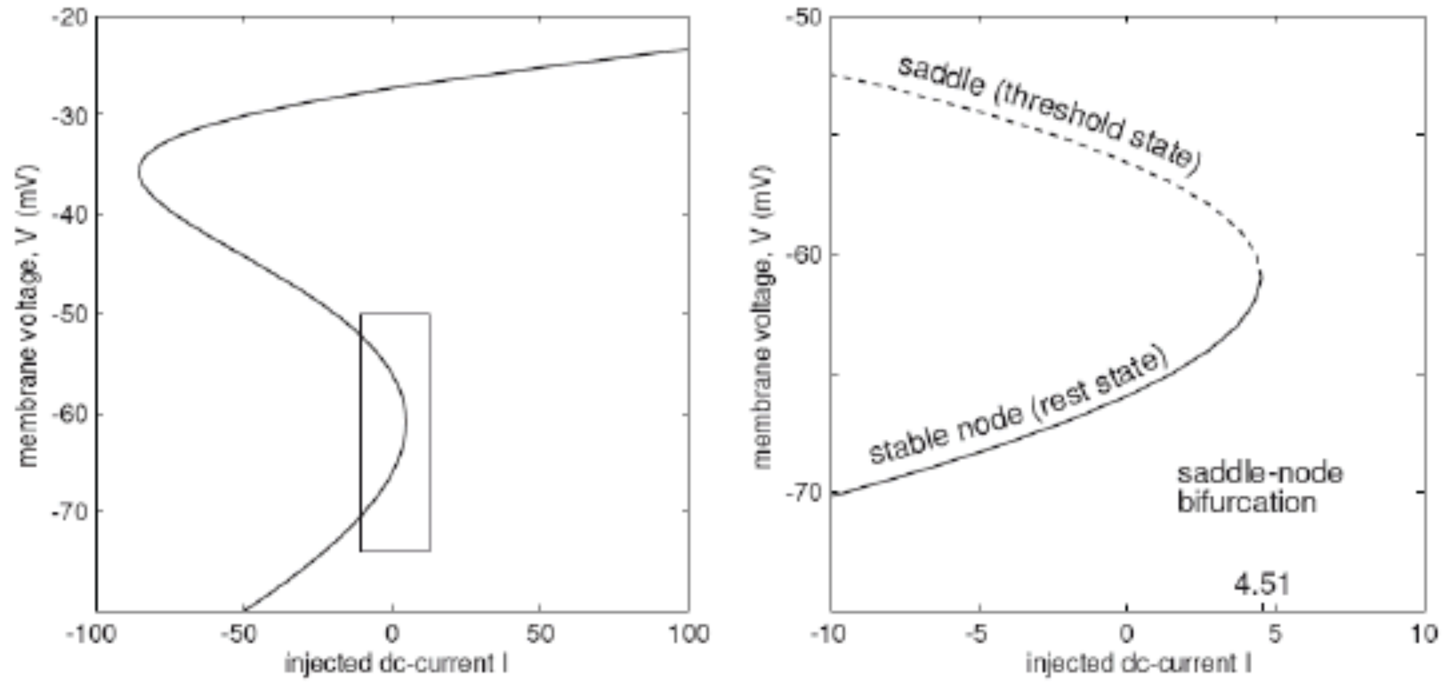

Two-dimensional neural models

- Saddle-node bifurcation in the $I_{na,p} + I_K$ model

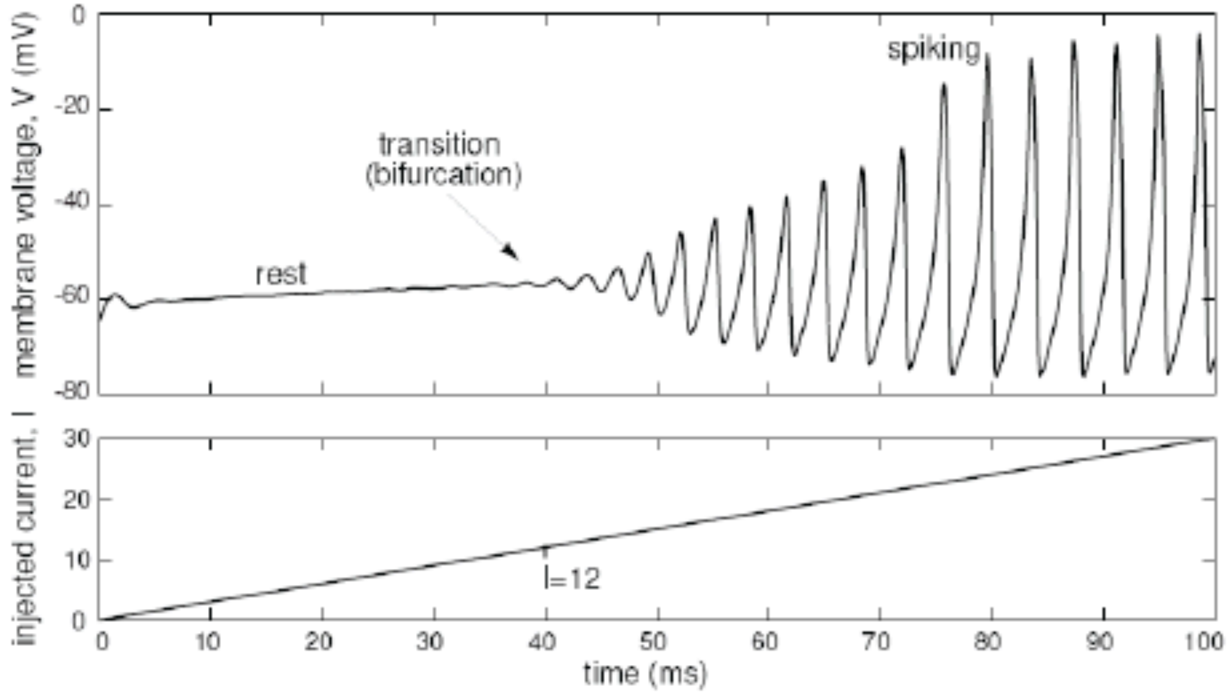

Figure 4.33: Transition from rest state to repetitive spiking in the $I_{Na,p}+I_K$-model with ramp injected current I; see also Fig. 4.34 (small-amplitude noise is added to the model to mask the slow passage effect). Notice that the frequency of spiking is relatively constant for a wide range of injected current.

Two-dimensional neural models

- Supercritical Hopf bifurcation in the $I_{na,p}$ + I_K model with low-threshold K^+ current when I=12

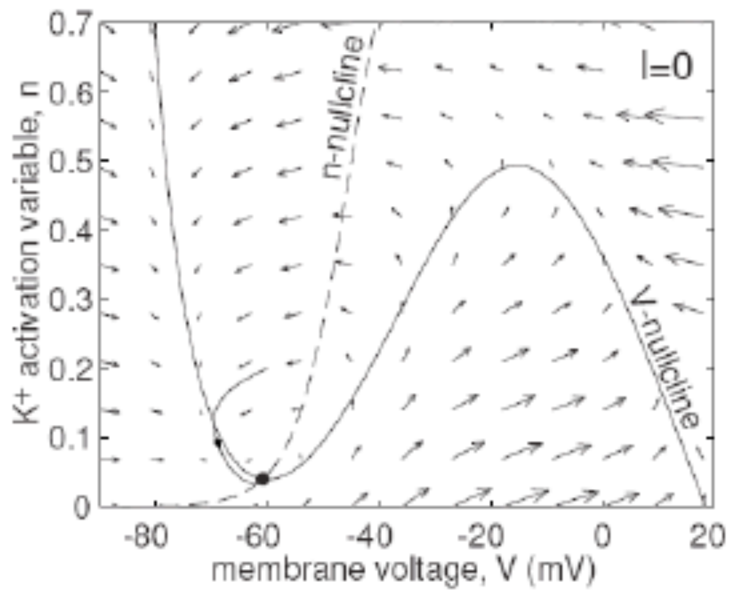

Two-dimensional neural models

- Supercritical Hopf bifurcation in the $I_{na,p} + I_K$ model with low-threshold K^+ current when I=12

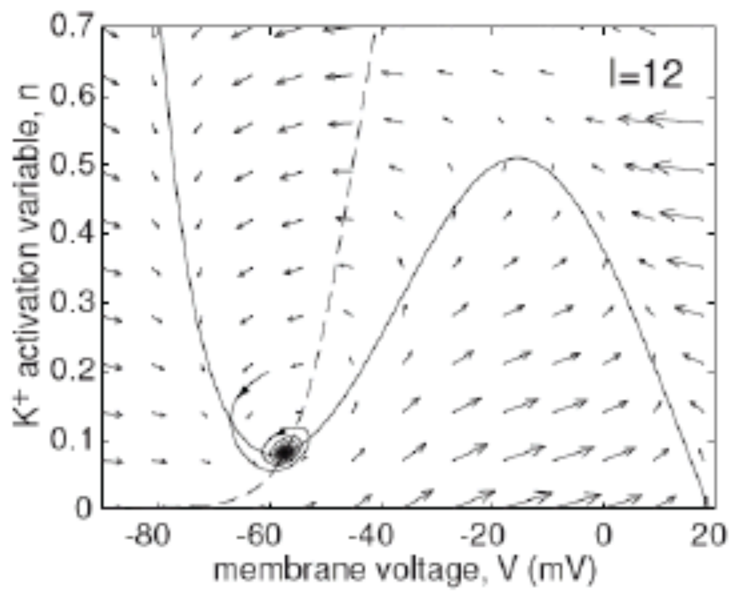

Two-dimensional neural models

- Supercritical Hopf bifurcation in the $I_{na,p} + I_K$ model with low-threshold K^+ current when I=12

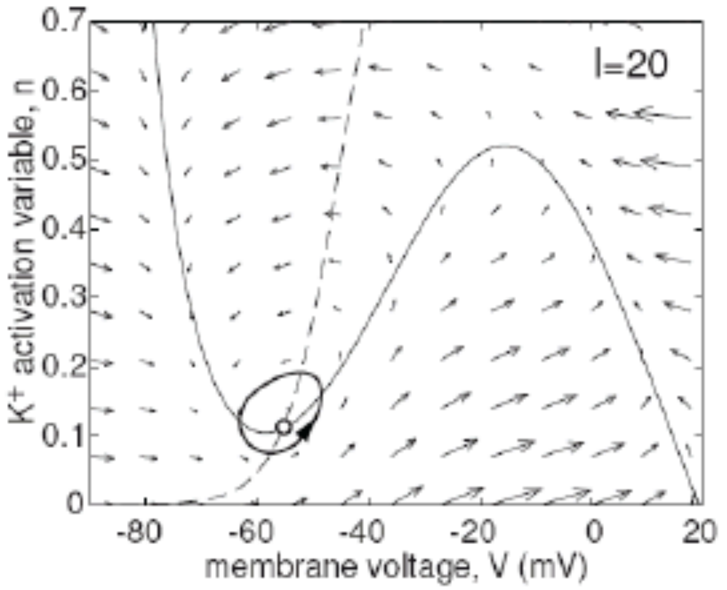

Two-dimensional neural models

- Supercritical Hopf bifurcation in the $I_{na,p} + I_K$ model with low-threshold K^+ current when I=12

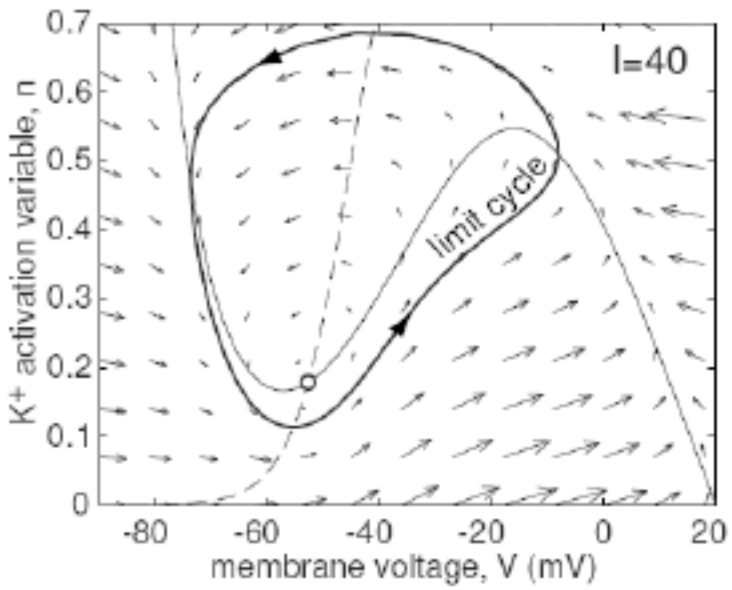

Two-dimensional neural models

- Supercritical Hopf bifurcation in the $I_{na,p} + I_K$ model with low-threshold K^+ current when I=12

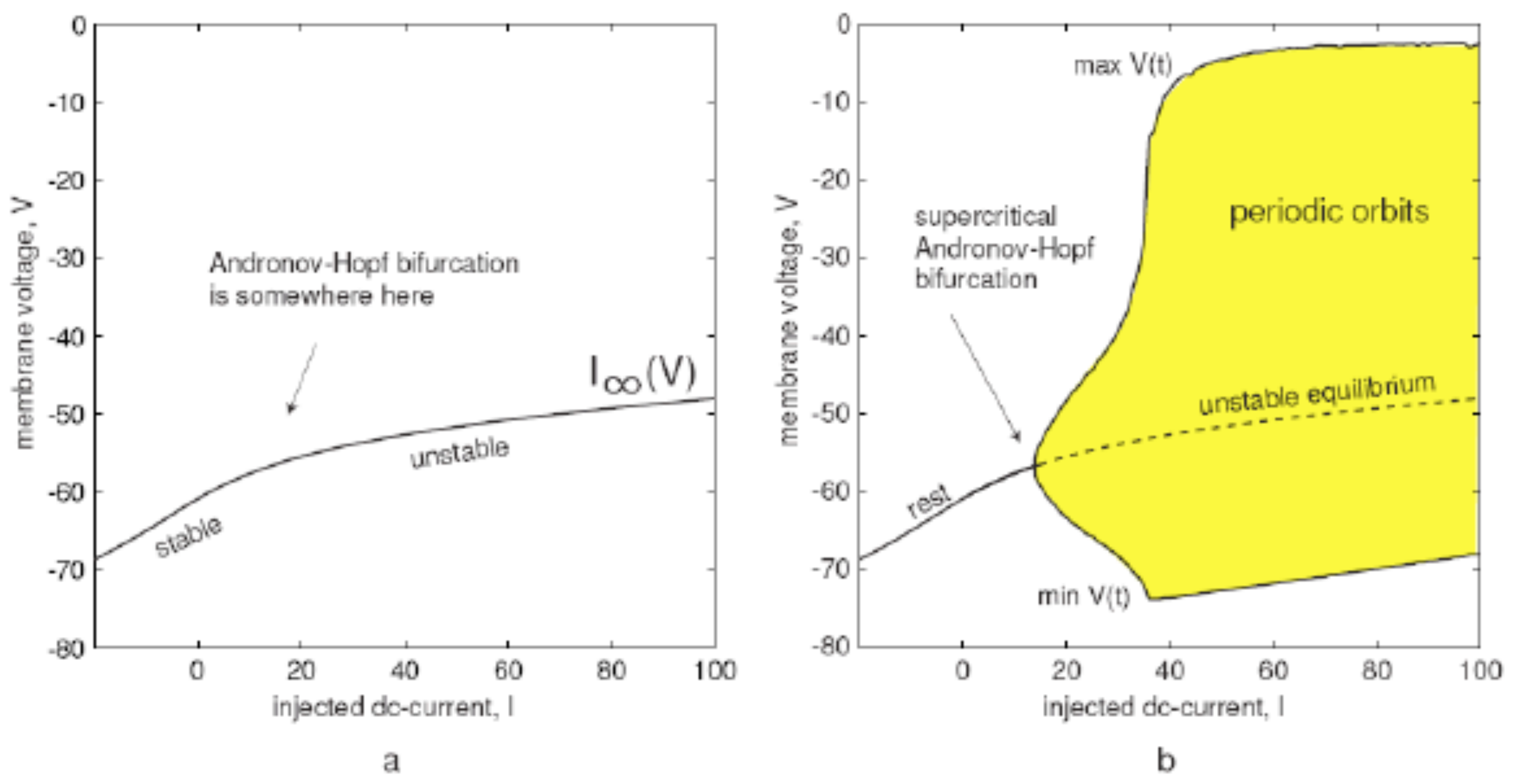

Two-dimensional neural models

- Supercritical Hopf bifurcation

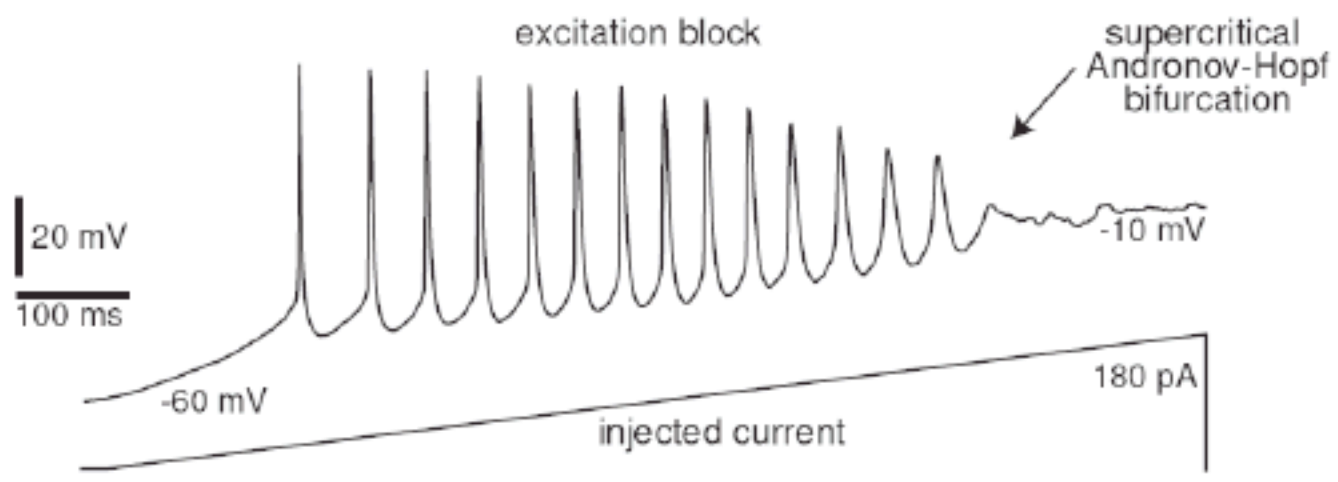

Excitation block in layer 5 pyramidal neuron of rat's visual cortex as the amplitude of the injected current ramps up

Two-dimensional neural models

- Supercritical Hopf bifurcation in the $I_{na,p} + I_K$ model

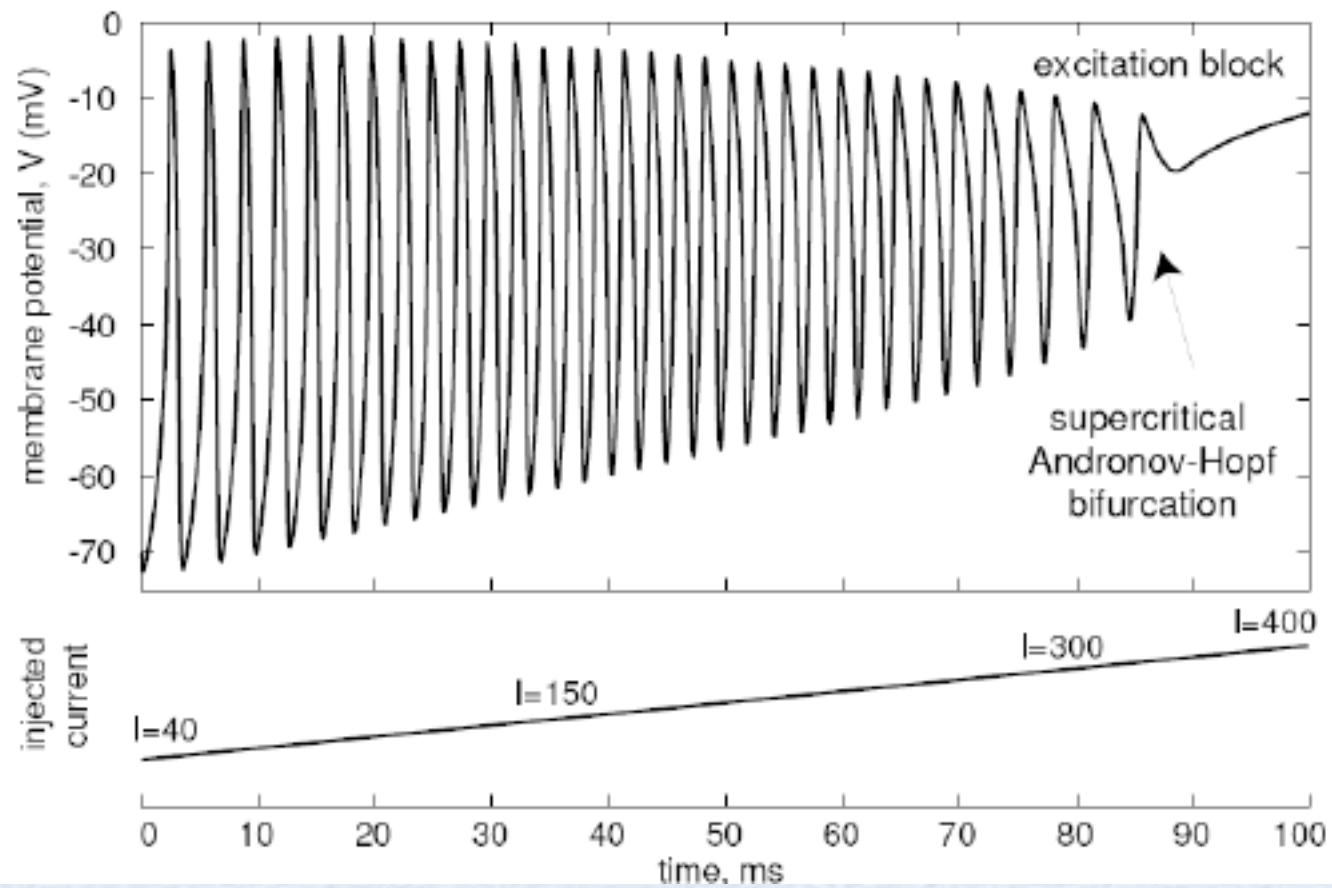

Two-dimensional neural models

- Supercritical Hopf bifurcation in the $I_{na,p} + I_K$ model

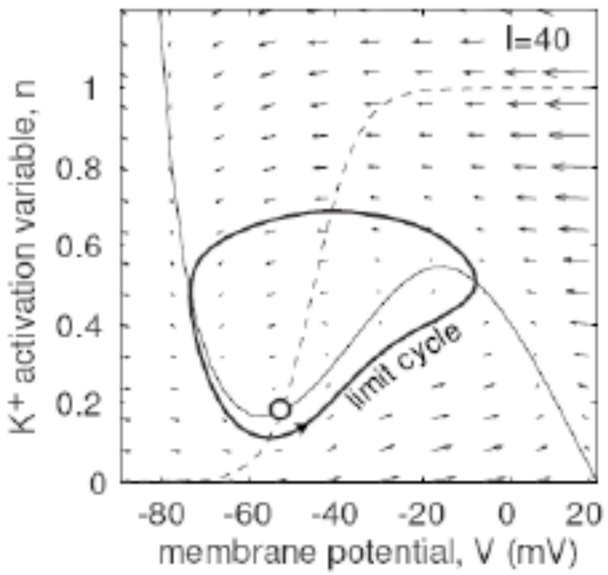

Excitation block in the $I_{Na,p}+I_K$-model: As the magnitude of the injected current I ramps up, the spiking stops

Two-dimensional neural models

- Supercritical Hopf bifurcation in the $I_{na,p} + I_K$ model

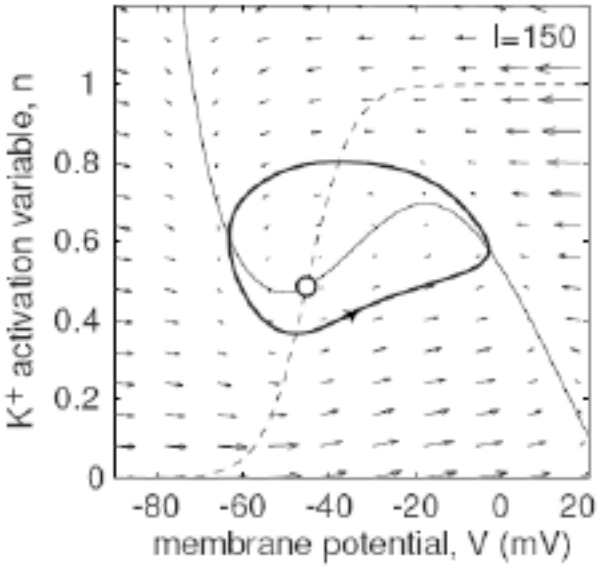

Excitation block in the $I_{Na,p}+I_K$-model: As the magnitude of the injected current I ramps up, the spiking stops

Two-dimensional neural models

- Supercritical Hopf bifurcation in the $I_{na,p} + I_K$ model

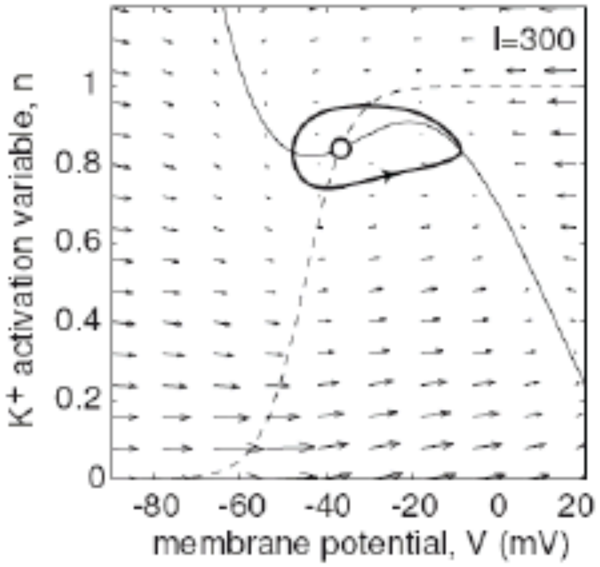

Excitation block in the $I_{Na,p}+I_K$-model: As the magnitude of the injected current I ramps up, the spiking stops

Two-dimensional neural models

- Supercritical Hopf bifurcation in the $I_{na,p}$ + I_K model

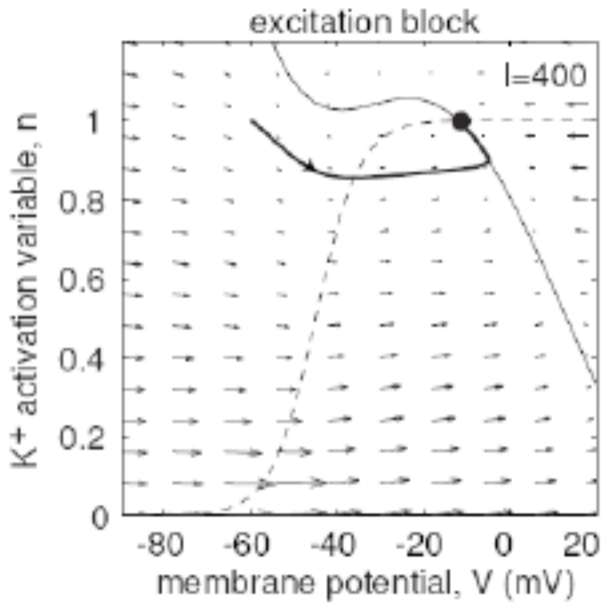

Excitation block in the $I_{Na,p}+I_K$-model: As the magnitude of the injected current I ramps up, the spiking stops

Aug24-11